IEEE Access
Multidisciplinary ⋮ Rapid Review ⋮ Open Access Journal

Received 15 June 2024, accepted 12 August 2024, date of publication 16 August 2024, date of current version 26 August 2024.

Digital Object Identifier 10.1109/ACCESS.2024.3444735

RESEARCH ARTICLE

Demand Estimation for Electric Vehicle Charging Infrastructure: An Extensive Approach Method

JOSÉ CALIXTO LOPES, (Member, IEEE), THALES SOUSA, (Senior Member, IEEE), AND JOEL D. MELO, (Senior Member, IEEE)

Center of Engineering, Modeling and Applied Social Sciences, Federal University of ABC, Santo André, São Paulo 09210-560, Brazil

Corresponding author: Thales Sousa (thales.sousa@ufabc.edu.br)

This work was supported in part by Neoenergia Group (In the scope of the project "Green Corridor for Hybrid and Electric Vehicles" under process 23006.001802/2019-09), in part by Brazilian Electricity Regulatory Agency (ANEEL), in part by the Federal University of ABC (UFABC), in part by the Coordination for the Improvement of Higher Education Personnel (CAPES) under Finance Code 001, in part by the Brazilian National Council for Scientific and Technological Development (CNPq) under Grant 407244/2023-9, in part by the São Paulo Research Foundation (FAPESP) under Grant 2021/08832-1, and in part by the National Institute of Science and Technology of Electric Energy - Brazil (INCT - INERGE).

ABSTRACT Urban planning must coordinate expanding public electric vehicle charging infrastructure (EV-CI) with energy distribution companies to satisfy growing demand. To this end, measurements and charger load curves are indispensable to execute appropriate operational studies and expansion planning. However, the necessary databases are small in cities with low EV penetration, and may not adequately characterize future consumption patterns. This article proposes an "Extensive Method for Demand Estimation in Charging Infrastructures" (X-Modeci) to fill this gap, which is especially beneficial for large metropolitan areas. The method employs statistical regressions to model the different phases of EV adoption, using traffic simulations to incorporate new travel dynamics that may arise due to increased charging and new EV battery range values. The proposal result is a spatial database that shows EV-CI load curves for typical urban traffic days in locations that would be more appropriate for installing new chargers. This results class can help energy companies identify the best connection locations and necessary reinforcements in the distribution grid to meet electromobility demand. The method was applied in the most significant capital in the Northeast of Brazil, showing that the estimated load curves tend to reach their maximum point between the end of the afternoon and the beginning of the night, following the high rate of vehicle circulation during this period. The case study clarified that the characterization of EV-CI use provided a 10% gain in the EV-CI usage rate about the national average, respecting regulated levels. In this way, the results of the proposed method can help the agents involved better understand the energy demand within the scope of electromobility plans with high spatial resolution at the location of the main avenues in urban areas.

INDEX TERMS Electric vehicle, electromobility, energy consumption, load curves estimation, power distribution system planning, public charging stations.

I. INTRODUCTION

The Electric Vehicles (EV) global fleet reached 40 million units in 2023, and the market to waiting to sell 17 million in 2024 [1], showing the exponential progress of electromobility. On the other hand, as the electrification march advances, an Electric Vehicle Charging Infrastructure (EV-CI) with fast chargers and publicly accessible is essential to achieve similarity with conventional refueling [2].

EV-CI offers significantly shorter charging times than home charging as it employs chargers with high-rated power (above 10 kW and already exceeding 200 kW). Nevertheless, this fact imposes additional concerns for the planning and expanding energy distribution systems. With the electrification of the transport sector, the load will penetrate in an accelerated and random manner, increasing peak demand

The associate editor coordinating the review of this manuscript and approving it for publication was Mehdi Bagheri.

and imposing disorderly fluctuations in the load curve [3], [4].

EV charging is entirely different from the regular pattern in the industrial and residential sectors because of high volatility and fluctuating aspects. The leading causes are consumption dynamics, the disruptive pattern, and the spatial dispersion between drivers and chargers. These represent more challenges for urban and energy planners, considering the risk of congestion and compromising the electrical system's reliability [5].

In this context, load curve estimation emerges because it contributes to formulating appropriate plans that guarantee the market's sustainability and a harmonious relationship between energy and transport systems. The distribution planner must consider the possibility of simultaneous heavy grid usage and changes in peak demand when examining its assets, determining appropriate feeder and transformer sizes, and suggesting upgrades [6], [7]. Serious consequences can result from non-compliance with these factors, such as an imbalance in the supply-demand relationship and an increased probability of system collapse [8]. Furthermore, it is necessary to reduce investment costs in grid reinforcements based only on peak periods of high simultaneity [4].

However, modeling energy demand and estimating load curves for EV charging (although it is one of the solutions for planning modern energy systems) is problematic for many reasons. The load duration changes the travel time, drivers' route planning, and traffic flow patterns [8]. Furthermore, there are intrinsic spatio-temporal conditions, especially in regions in the EV-CI expansion phase where charging is even more stochastic [9].

Measurement campaigns can only be effective when the fleet and EV-CI stabilize. Until then, databases are minor and can inadequately characterize load dynamics. Therefore, techniques based on data analysis are not helpful in these cases, as the prevalence of charging is minimal or non-existent, and more chargers are needed to carry out conclusive measurements. Additionally, although there has been excellent progress in the use of data science, obstacles related to privacy laws restrict the data availability and applicability of these techniques.

A. APPLICATIONS AND CONTRIBUTIONS

The Extensive Method for Demand Estimation in Charging Infrastructures (*X-Modeci*) proposed in this article addresses the estimating load curves problem and determines the demand profile for public charging for each EV penetration level while considering the drivers' spatial dispersion.

The *X-Modeci* comprises five modules and distinguishing characteristics not found in the available literature. Refer to Section II-B for further details. Nonetheless, five of these differentiating features can be condensed as follows: 1) the study examines the potential adopters market of EVs and addresses the heterogeneous spatial distribution of drivers; 2) it takes into account the dynamics of urban traffic, characterizing the various stages of adoption and use; 3) it considers the State of Charge (SOC) of the battery; 4) also takes into account the precise geographical location of each charging point and 5) real public access data was used.

The main target of the proposal (although there are others) is distribution companies. The method's essence is to provide inputs to complement analyses in the system planning stages and grid access request cases. The aim is to mitigate impacts related to uncertainties regarding the dynamism of EV penetration growth. The spatial estimation of demand is crucial for several reasons, including the connection's dependency on the electrical grid and the comparison with residential, industrial, commercial, and other load curves [3]. Moreover, with the calculation of maximum demand, it becomes possible to recognize peak periods, which can assist in determining whether the electricity grid can handle new loads or if there is a need to increase capacity or feeders.

From input data to outputs, databases and results are modeled spatially via Geographic Information Systems (GIS). Spatial databases facilitate the development of thematic maps that visually depict information at all planning stages, as previously demonstrated in [10]. Georeferenced maps include identifying the most appropriate locations for installing charging points. The proposal allows integration with urban and energy planning tools, land use, and topography mapping. In addition to demand, the proposal offers hourly load curves, peak hours, and typical factors contributing to charging station connection studies.

The main contributions, while not limited to these, can be summarized as follows:

- The *X-Modeci* considers the EV fleet's dynamic growth and EV drivers' travel patterns based on statistical regressions and transport flow simulation. Thus, the increase in load density can be better characterized, especially in large metropolitan areas;
- Load curves are estimated by statistical modeling and considering the EV adoption stage and diffusion in addition to the real urban traffic dynamics and travel patterns. The method provides a spatial database with load curves for the entire EV-CI, considering different levels of EV penetration;
- Power Distribution System (PDS) calculations elucidate new utilization factors in electrical installations, considering the demand for charging increases. Energy distributors can use *X-Modeci* to assess the impacts and uncertainties of each penetration scenario when receiving requests to connect the new electric vehicle charging station.

II. LITERATURE REVIEW

A. RELATED WORK

Some approaches to the problem of estimating charging station load curves are based on data analysis techniques (big data, deep learning, machine learning, etc.), which always require the availability of historical series. The authors

focus on obtaining annual energy consumption, and the methodologies selected would depend on the context and purpose of each model. In [11], planning is approached from an optimization model that includes grid operation and user preference factors. The focus given by [12] is on load prediction through the massive application of deep learning techniques. As with [12], [13] used time series-based methods to forecast demand. Likewise, a procedure to identify typical large-scale loading profiles was proposed by [14].

However, the solutions mentioned above did not consider the possibility of the unavailability of historical loading data. Furthermore, they require complex modeling, parameter adjustment, and multiple data sources, making implementation difficult. Although there are countries with mature EV-CI, in most parts of the world, electrification is still in an early stage of development. Therefore, they do not have a consolidated market and cannot adopt this approach. Another severe limitation of these studies is access to data, which modern privacy policies have increasingly restricted. Furthermore, the proposals do not incorporate either EV stochastic or traffic flow behavior.

Recently, some authors have designed the load curve based on a traffic simulation result, considering the spatial-temporal aspect and hourly and daily vehicle flow variations. In [15], the location of buyers, the number of EVs, and demand were estimated. The [16] approach is similar, but several simplifications had to be imposed, limiting applicability to small locations. The non-linear programming model is developed in [17] and considers demand, utility, and battery characteristics. In [18], the estimated load curves are superimposed to obtain the overall curve. The demand variability and peak load were predicted in [19] by formulating an optimization problem. Finally, in [20], the estimation process is based on traffic information and highway patterns.

The above approaches gain prominence compared to those based on data, but they assume that travel patterns are fixed throughout the journey. Therefore, they fail to consider that the need for charging on route completely changes this pattern, imposing volatile behavior on the driver's driving modes. Considering exogenous factors, such as seasonality in route selection and the influence on traffic conditions, is one of the gaps in improving the granularity in generating load curves.

B. DISCUSSIONS AND PROPOSED INNOVATIONS

Few proposals have considered the different stages of electric mobility (purchase, modes of use, travel behavior, and charging). Among these, it is assumed that charging patterns will remain unchanged for any level of EV penetration. However, the increase in the fleet implies a greater EV-CI, bringing more route options to the driver. Therefore, it must be considered that future scenarios will change the route choice and, consequently, the load curves. In contrast to previous works in the literature, *X-Modeci* considers the variation in penetration in future scenarios, which promotes more excellent quality in the estimates.

A deficiency of the proposals analyzed is the lack of a joint analysis involving transport and energy systems, which must be addressed as they are related. On the one hand, the location of property owners and travel patterns affect urban flows. On the other hand, the spatial distribution of charging points and SOCs changes the operation and planning of the electrical grid [21], [22]. Therefore, an innovation of *X-Modeci* is a holistic vision, from modeling urban traffic, its dynamics, and routes to the need for charging batteries [8].

Most authors characterize load curves based on the behavior of a small set of charging stations. Few studies can estimate load curves in a large region (from neighborhoods to entire cities). Studies have only been able to demonstrate their contributions in small, fractional, or test networks, which is an obstacle to replication in large metropolitan areas [16], [19]. To overcome these limitations, *X-Modeci* focuses heavily on large-scale applications, making it possible to integrate analyses into a single solution within the co-simulation concept [23].

Considering the preliminary discussions, *X-Modeci* helps distribution agents plan to meet growing load demand and deal with the significant change in load balancing dynamics. One of the intrinsic novelties is the possibility of analyzing peak load times, maximum demand values, and typical factors that characterize the behavior of the EV-CI in aspects such as homogeneity (the distribution of use between periods of the day) and simultaneity /coincidence (power required at the exact moment). In this sense, to the best of the authors' knowledge, no published study has considered all these assumptions together.

III. EXTENSIVE METHOD FOR DEMAND ESTIMATION IN CHARGING INFRASTRUCTURES (X-MODECI)

The *X-Modeci* consists of five blocks, where a hierarchical relationship diagram is in Fig. 1, and is detailed in Fig. 2. The main highlight of the proposal about others found in the literature is that it makes it possible to characterize the growth of load density in future scenarios. In this sense, a relevant contribution is the possibility of estimating load curves to assist distribution companies in connection analysis studies for new charging stations and in planning reinforcements in the electrical system infrastructure. Another benefit of the work is the possibility of considering the different EV stages of adoption and use, improving the quality of the planner's analyses.

Block 1 (Section IV-A) applies statistical techniques to estimate the spatial distribution of EV adopters. The modeling characterizes the evolution of fleet growth dynamics, providing the driver's location and the starting points of EV travel. Spatial econometrics is developed, and regression models are applied to estimate the adoption rate and obtain a database on the geographic location of each driver.

X-Modeci stands out compared to other studies for characterizing the interdependent relationship between transport

and energy grid. In this sense, transport modeling contributes to determining the EV driver's behavior, which differs from the standard behavior of the driver of a combustion vehicle. In this sense, in Block 2 (Section IV-B), a transport simulation determines the travel dynamics, and an algorithm calculates the SOC for use in determining EV-CI and calculating demand in subsequent blocks.

Block 3 (Section IV-C) uses the Location-Allocation Problem (LAP) approach to determine the necessary EV-CI to meet demand. An algorithm based on graph theory proved suitable for optimizing the allocation and can be adjusted according to the planner's needs. A location ideal for installing a charging station, it has more significant EV movement and a low charge in their batteries. Consequently, the best locations for installation are selected considering the need to meet the growing demand for EV charging.

In Block 4 (Section IV-D), an algorithm based on the Route Choice Problem (RCP) directs the EVs for charging points, calculates routes considering the shortest path, and updates the SOC. An output database summarizes the number of vehicles directed to each charging station and the SOC of each one. Therefore, it is possible to determine the expected energy consumption, which will also be used in the next block.

It is difficult to predict the electrical demand behavior at a time when EV penetration is still low or non-existent. Therefore, Block 5 (Section IV-E) completes the *X-Modeci*, aiming to identify, graphically and spatially, any need for grid reinforcement by identifying peak periods throughout a typical day. Hourly demand curves and factors related to load behavior are estimated for each charging point of EV-CI. In the final output, a spatial database is obtained with a demand estimate for installed chargers considering different penetration levels.

A. INPUT DATA

- **Sociodemographic** (*inpIV-A, Block 1*): they are public, can be obtained from government agencies, and contain variables related to the demographic census, such as maps of territorial division, age, education, and income. They are usually segmented into sub-regions, known as census sectors, and made available in layers of information that can be processed in GIS. Economic data, such as vehicle prices, energy tariffs, fuel prices, taxes, and nominal interest rates, are also considered.
- **Urban Mobility** (*inpIV-B*, Block 1 and Block 2): also publicly available and includes maps that divide the area into traffic zones (ZT) and origin-destination matrices (OD). The information is grouped in tables that summarize the travel distribution for each hour of the day and during peak periods. This data is used to characterize travel demand and enable traffic simulations. They form part of urban planning studies and provide insights into traffic patterns and trends for regions worldwide [24].

B. PRELIMINARY DATA

- **EV adopters and OD Matrix** (*outV-B*, Block 1): indicates the locations of the drivers, the sectors in which they are located, and the OD matrices of the EVs;
- **Flow and SOC** (*outV-C*, Block 2): determines driving patterns, driver preferences, and battery status;
- **EV-CI location** (*outV-D*, Block 3): determines the spatial location of each charging point, which can each have one or more, fast (AC) or ultra-fast (DC) chargers;
- **Energy expectation** (*outV-E*, Block 4): compiles the number of EVs at each charging point and updates the SOC of each one, providing the amount of energy (Watt-hours) needed to meet demand;

C. OUTPUT DATA

- **Demand and Factors** (*outV-F*, Block 5): represents the final results with the characterization of the hourly demand (in watts), reached by the load curve, for each point; the maximum demand, the average demand, and the coincident and non-coincident demand are provided; four typical factors are calculated: diversity, coincidence (or simultaneity), demand and load; each block results are compiled in a final database and can be processed a posteriori in any GIS system.

IV. X-MODECI USED TECHNIQUES

A. BLOCK 1: DRIVER'S CLUSTER

The pattern of behavior of EV adoption rate depends on geographical, socio-economic, and cultural factors peculiar to each region [21]. This block links these factors and is based on the diffusion of innovations theory developed by Everett Rogers found in [25]. Because of the high cost, EV drivers tend to conglomerate in a dispersed manner, characterizing heterogeneous behavior in their spatial distribution. The first adopters will influence the neighborhood over time, triggering the future diffusion of EVs [26]. The objective of this block is to estimate the starting point of EV travel based on the characterization of the evolution of the rate of EV adopters. In Block 2 (Section IV-B), this estimate is associated with the OD matrices and feeds the transport modeling proposed.

1) SPATIAL ECONOMETRICS

a: HIERARCHICAL SPATIAL AUTOREGRESSIVE MODEL (HSAR)

The proposed method characterizes the dynamic growth of possible travel EV starting locations. In this sense, based on an initial rate (which may be available from the distribution company or traffic control bodies), the HSAR model determines the proliferation of adopters. It considers the spatial influence of neighboring areas (group dependence effect) based on socio-demographic variables [27]. Then, the model updates the initial rate, making it possible to characterize the heterogeneous distribution and determine the

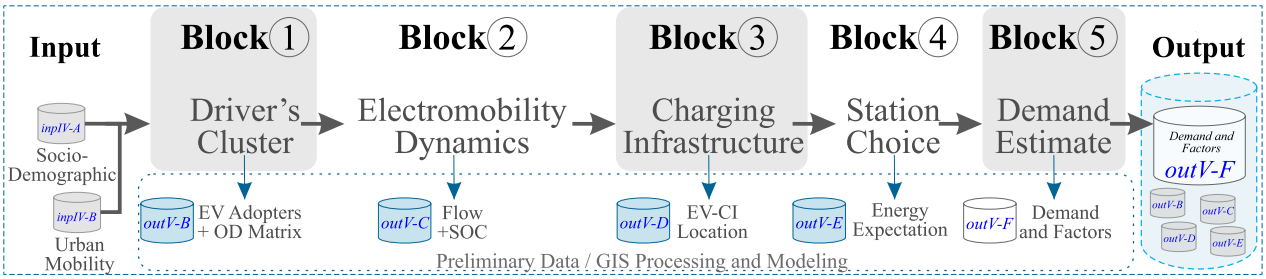

FIGURE 1. X-Modeci algorithm flowchart - overview.

market of adopters and its dynamism, according to (1) [28].

$$y_{i,j} = \rho W Y_{i,j} + \beta X_{i,j} + \gamma Z_{i,j} + \Delta\theta_{i,j} + \xi_{i,j} \quad (1)$$

where ρ is the coefficient for the global spatial iteration; W is the matrix of spatial weights that measures the influence between sub-regions i, j; Y is the initial rate of adopters; $X_{i,j}$ and $Z_{i,j}$ characterize the socioeconomic variables; β and γ are regression coefficients; Δ is the random number weight matrix that allows describing the stochastic nature of adopters, with $\theta_{i,j}$ calculated for different levels and $\xi_{i,j}$ characterizing the stochastic nature related to the purchase.

b: LOGISTIC REGRESSION MODEL (LR)

As explained, the diffusion of EVs has a heterogeneous behavior and is difficult to predict, as it varies depending on socioeconomic factors. In this sense, the combination of HSAR and LR techniques makes it possible to characterize the growth profile, considering intrinsic uncertainty factors adequately. The LR identifies new regions with profiles for acquisition and determines the evolution of the EV adopter rates over the planning horizon. An iterative sequence is reproduced using new output data from a previous scenario and employing it as input for the next one. Finally, the spatial distribution of adopters for each sub-region is obtained, considering penetration rates. Equation (2) is used to determine the cumulative diffusion distribution function (F_t) [29]:

$$F_t = \frac{1 - e^{-(p+q)t}}{1 + \frac{q}{p} e^{-(p+q)t}} \quad (2)$$

Equation (2) calculates the probability of adopting an EV over the planning horizon (t), considering the innovation (p) and imitation (q) coefficients, which represent the external and internal influences of diffusion.

B. BLOCK 2: ELECTROMOBILITY DYNAMICS

The *X-Modeci* can associate the spatially dispersed penetration of adopters (described in Block 1, Section IV-A) with the dynamics of their travels. These dynamics were determined from traffic simulations using the software *Aimsun* software [30]. Travel dynamics are characterized by the flow and SOC of EVs on the roads in the study region. Traffic flow (Section IV-B1) is defined as the number of vehicles circulating on a given street in a period [31]. The SOC (Section IV-B2) represents the residual energy of the EV's battery, considering that it employs power from its batteries as it moves.

1) TRAFFIC SIMULATION

a: TRAFFIC ZONES AND CENTROIDS

The study area is divided into sub-regions, as done in census studies. They group socio-economic and behavioral characteristics of the population, allowing the understanding of the trips produced and attracted within the zone [24]. Each one is given a centroid to assign points of generation and absorption of vehicle flows and to characterize the transport demand.

b: TRANSPORTATION NETWORK

A transportation (or traffic) network is a graph that represents a geographic space and models the infrastructure that allows different modes of transportation to move around [31]. In this graph, the vertices (or nodes) represent the intersections/crossings, and the edges (or links), the urban roads. It can be modeled by integrating the *Aimsun* [30] and a georeferenced Open Street Map (OSM) database [32], easily obtained from the Internet.

c: OD MATRIX, DEMAND, AND MESOSCOPIC SIMULATIONS

The OD matrix is associated with ZTs (Section IV-B1a): each trip's start and end points are specified. In the matrix, each cell represents the connection points of a journey, (i.e., from an origin to a destination), and the number of trips made [24]. The spatial database obtained in Block 1 (Section IV-A) is integrated into this modeling point for composing scenarios.

The *X-Modeci* uses real traffic data and, in addition to EVs, other transportation modes are characterized (conventional vehicles, motorcycles, public transportation, etc.). The matrices are applied to parameterize the traffic demand, and then calibration and validation steps are carried out to allow mesoscopic traffic simulations [24], [31].

2) SOC ALGORITHM

a: ENERGY CONSUMPTION MODELING

As with traffic simulation (Section IV-B1), the SOC must be expressed for each road considering its route. The energy

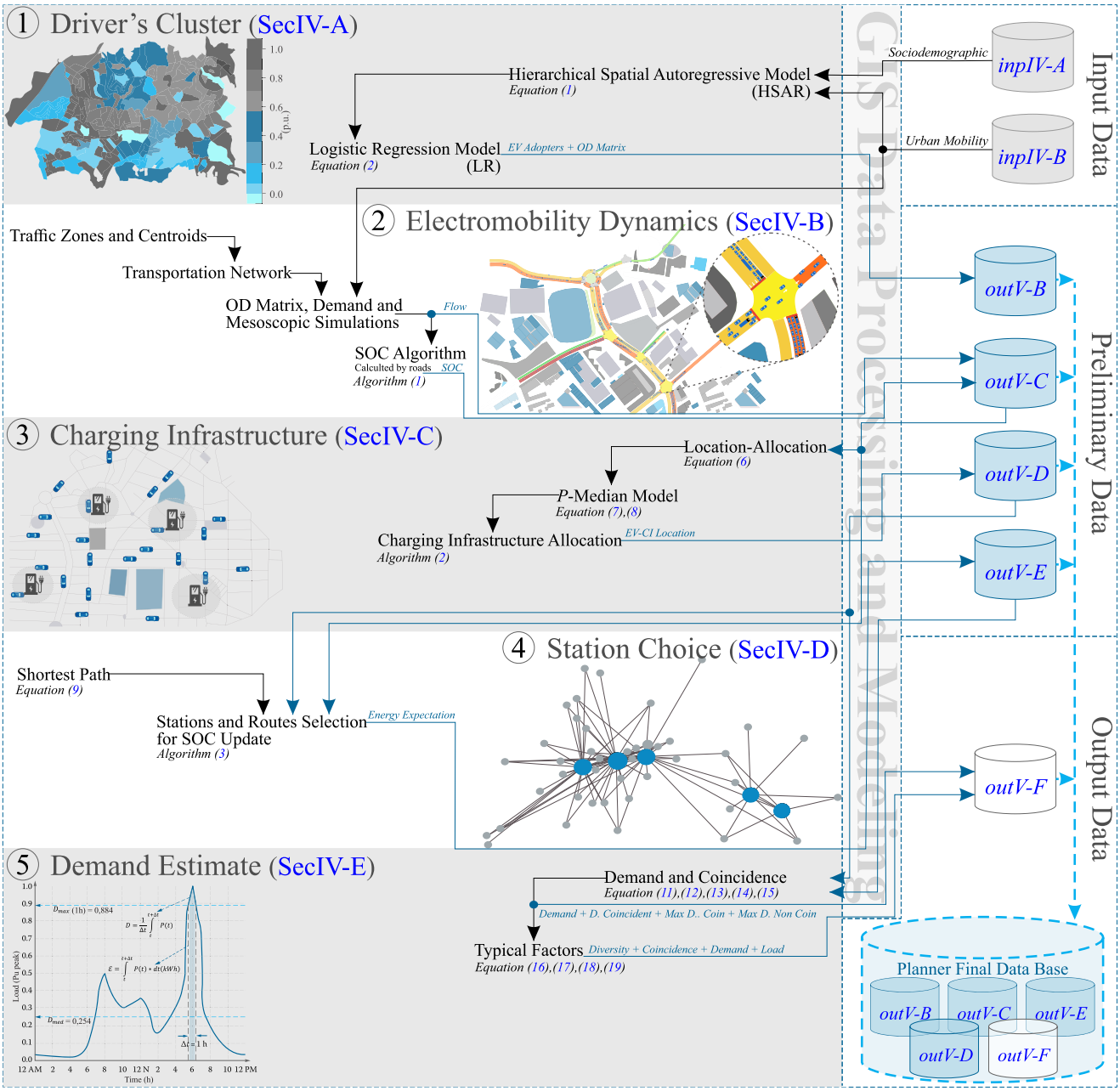

FIGURE 2. X-Modeci algorithm flowchart - detailed view.

consumption of an EV is calculated in 3 steps: 1) power demanded in the i, j segment; 2) consumption on the i, j segment, and 3) updated remaining SOC considering the consumption on the i, j segment.

The relationship that calculates the mechanical power required by the EV is given by (3), according to modeling provided by [33]. In this relationship, the power demanded is calculated for the route of a given segment, which is why it is noted in the equation as $P_{i,j}$. A segment corresponds to a street, avenue, lane, etc, through which the vehicle moved. The [33] proposed the modeling fundamentals, and details regarding its application were previously covered and deepened in [34].

$$P_{i,j} = \left(\frac{1}{2} C_d \rho A v_{i,j}^2 + mg \sin\alpha + C_r \cos\alpha\right) \vec{v_{i,j}}^2 \quad (3)$$

where $P_{i,j}$ is the power demanded in the path between a point i and an end j; C_d the aerodynamic drag coefficient; ρ the air density; A the front area of the vehicle; $v_{i,j}$ the speed of the car in a segment (obtained from traffic simulation); m the mass of the vehicle; g the gravitational constant; α the slope and C_r the coefficient of rolling resistance.

Consumption is also calculated for each street where the vehicle travels, as (4). There are two relationships to

be considered in consumption: when $P_{i,j} \geq 0$ is more significant than zero, the vehicle is consuming energy, therefore operating in engine mode; otherwise, if $P_{i,j} \leq 0$, it is producing power by the regenerative braking system, through the generator mode.

$$b_{i,j} = \begin{cases} \phi^d \varphi^d P_{i,j} t_{i,j} & \text{if } P_{i,j} \geq 0\ kW \\ \phi^r \varphi^r P_{i,j} t_{i,j} & \text{if } P_{i,j} \leq 0\ kW \end{cases} \quad (4)$$

where $b_{i,j}$ corresponds to the consumption of energy in the path between a point i and a point j; ϕ^d represents the regression coefficient for electric motor efficiency (engine mode); φ^d the regression coefficient for electric motor efficiency (engine mode); ϕ^r the regression coefficient for electric motor efficiency (generator mode); φ^r the regression coefficient for battery efficiency (generator mode) and $t_{i,j}$ the time taken to travel a segment (obtained from traffic simulation).

Finally, to obtain the percentage SOC on each street (SOC_{act}), (5) is applied. The first term is used for the first segment and the second for others.

$$SOC_{act} = \begin{cases} \frac{SOC_{int} - b_{i,j}}{B} 100 & \text{for } 1th \text{ section} \\ \frac{SOC_{i,j} - b_{i,n}}{B} 100 & \text{for } n' \text{ section} \end{cases} \quad (5)$$

where SOC_{int} is the initial SOC of the vehicle when leaving its origin (characterized by a random seed adjustment), and B is the EV battery capacity. A previous work further developed the ideation for the SOC calculation [34].

b: COMPUTATIONAL IMPLEMENTATION

Algorithm 1 shows the steps for calculating the SOC. Initially, the data is manipulated to retrieve each vehicle's trajectory, time, and speed by section (street, avenue, etc.). The information is stored in an initial data frame. On line 1, each EV is assigned an initial SOC value (randomly characterized and varying between a range that can be pre-configured). Lines 2 to 15 set up the repeating loop to calculate energy consumption for each vehicle and in each section. During its journey, the SOC is updated until it reaches its destination or until it reaches the minimum limit (SOC_{min} is a sensitive and parameterizable variable, which determines when the loop stops in line 9). The information is compiled, and the data frame is updated with the average SOC per section.

C. BLOCK 3: CHARGING INFRASTRUCTURE

This block is intended to estimate the EV-CI, which in most places is still evolving, making electrical planning analyses unfeasible. In this way, using traffic simulations as a pillar (Section IV-B), the goal is to identify promising locations within the region under study. The method identifies the best places for installing charging stations to meet the growing penetration of EVs. when the area has already established infrastructure, the location points can be georeferenced in GIS and used directly in Block 4 (Section IV-D).

Algorithm 1 SOC Calculation by Roads

Input: Aimsun's SQLite (Section IV-B1); EV data sheet; Variables and parameters

Output: Average SOC on each street in the region

Pre-Processing: collect data on vehicles, trajectories, sections, and times

Compute: section speed $\vec{v}_m = \frac{\vec{\Delta}_s}{\Delta_t}$

Create: Datafame ← compiled values where i is a trajectory of a set I and j is a section of a set J

1: SOC_{int} ← random seed SOC in a range
2: Initialize $i = 0$ and $j = 0$
3: **while** $i \leq J$ **do**
4: **for** each section in J **do**
5: **while** $j \leq J$ **do**
6: Step 1: Computes the power $P_{i,j}$ by (3)
7: Step 2: Computes the consumption $b_{i,j}$ by (4)
8: Step 2: Update SOC_{act} by (5)
9: **if** $SOC_{act} \leq SOC_{min}$ **then**
 Break
10: **end if**
11: $j \leftarrow j + 1$
12: **end while**
13: **end for**
14: $i \leftarrow i + 1$
15: **end while**
16: **return** Updated Dataframe

In practice, the places chosen to accommodate EV-CI are those with high EV movement, like parking lots, malls, and commercial areas, predominantly in more central regions [8], [35]. The proposal starts from this premise and establishes the most likely locations with high flow and low SOC considering the travel dynamics (Section IV-B).

1) LOCATION-ALLOCATION

When determining the best locations for installing chargers, the goal is to define the best access routes to meet drivers' demands. At the same time, one must comply with the planner's criteria and restrictions (good location, easy access, security, etc.) to improve the quality of service [35], [36].

The EV-CI was determined using the Location-Allocation Problem (LAP) [37], based on graph theory [38] and modeled by the p-Median Model (PMM) [39]. The objective is to determine the infrastructure in a way that efficiently supplies the demand points. The LAP concurrently determines suitable locations for installations and allocates demand points to the determined locations [37]. The points are strategically located to minimize the costs between demand and EV-CI, weighted by (6) to create a matrix of distances $W_{i,j}$. Each assigned point may have one or more fast (AC) or ultra-fast (DC) chargers.

$$f_{i,j} = \frac{\frac{d_{i,j}}{d_{i,j_{(max)}}}}{\frac{F_i}{F_{j_{(max)}}} + \frac{80 - SOC_i}{SOC_{j_{(max)}}}} \quad (6)$$

where $f_{i,j}$ is the weight function; $d_{i,j_{(max)}}$ is the maximum coverage distance from the point of EV-CI; F_i is the average flow of EVs; $F_{j_{(max)}}$ is the maximum flow that a station can handle; SOC_i average EV SOC on urban roads and $SOC_{j_{(max)}}$ is maximum SOC to be supplied by station.

a: P-MEDIAN MODEL BASIC STATEMENT

The search space for candidate solutions for the installation was formulated based on the PMM [39]. With it, it is possible to allocate a number p of installations, minimizing the distance and cost relationship from places with high demand (requesting vertex) to the closest installation (serving vertex), which improves service supply [40]. The model choice is justified by its wide use in situations where both the demands and candidate locations for installation are known [10].

The core of PMM is to define the location of p facilities (called medians) to satisfy all requirements according to (7) [39]. In other words, given two subsets of vertices of a graph $G = \{V, E\}$, one consisting of candidate facilities $V_P \in V$ and the other consisting of demand points $V_i \in V$ weighted by the function $f_{i,j}$ (according to (6)) and where E is the set of edges representing urban roads; select a subset of facilities V_P* such that the sum of the weighted distances from each $v_i \in V_I$ to the nearest $v_p \in V_P$ is minimized by (8) [10].

$$\sum_{i=1}^{V}(d_{vi,vp*})f_{i,p*} \leq \sum_{i=1}^{V}(d_{vi,vp})f_{i,p} \tag{7}$$

From this definition, the absolute median is the 1-median of G, with the V_P* vertices being called median vertices.

$$Z_{B3} = Min \sum_{i,j}^{V}(W_{i,j}) \tag{8}$$

b: COMPUTATIONAL IMPLEMENTATION

The PMM solution was based on the Teitz and Bart (TB) vertex substitution heuristic [40]. TB was chosen for its better computational performance compared to similar techniques, making it simultaneously possible to process solutions even in large graphics networks [10].

As described in Algorithm 2, at first, a cost matrix that weights all the facilities' V_P and the network's demand points (V_I) is generated. An initial set of random solutions (line 1) is selected and refined (see loop started in line 2) until the optimal solution is reached (when there are no more solutions to be tested, line 8). In line 3, one of the vertices (called v_k) is tested. As with all heuristics, a metric $\Delta_{i,k}$ is assigned to iterate the minimization calculations according to (8) (line 4). Finally, in the steps described between lines 5-8, the minimum weighted distance is sought at each iteration.

D. BLOCK 4: STATION CHOICE

On a day-to-day, an EV driver leaves his origin and heads towards a destination. It can go directly there if there is enough battery to reach it. If not, the route will need to be rerouted for charging. In this block, the database from Block 2 (Section IV-B1) is processed to select which EVs reach the minimum battery value SOC_{min} (variable configurable by the distribution planner and sensitive to the proposal). In these cases, the nearest station usually be the preferred choice for drivers [26], [35].

The output of this block compiles the number of EVs at each charging point (defined in Block 3, Section IV-C) and updates the SOC. This information can estimate the expected energy for the EV-CI being evaluated and is essential for calculating the electricity demand in the next block (Section IV-E).

Algorithm 2 Charging Infrastructure Allocation

Input: Average Flow and SOC (Section IV-B1)
Output: EV Charging Infrastructure Location
Implements: graph $G \leftarrow V, E$, and gets distance matrix $W_{i,j}$ weighted by $f_{i,j}$ (6)
1: $V_P \in V \leftarrow$ randomly selects candidate facilities
2: **while** there were not analyzed vertices **do**
3: Selects an untested vertex v_k;
4: Computes $\Delta_{i,k}$ by Z (8)
5: **if** $\Delta_{i,k} \leq Min\ \Delta_{i,1...i,2...i,n}$ **then**
6: *Replace*: v_k as the new lowest value vertex
7: *Classifies*: v_k as tested
8: *Inserts*: v_k into V_P
9: **end if**
10: **end while**
11: **return** Updated V_P as a set of EV Charging Infrastructure

1) STATIONS-ROUTES FOR SOC UPDATE

The development was based on an adaptation of the Shortest Path Problem (SPP) [24] and, as in Section IV-C, modeled using graph theory [38]. In this case, of the graph $G = \{V, E\}$, $V_P \in V$ is the set of EV-CI obtained previously, $V_{EV} \in V$ the set of EVs in need of charging and E correspond to urban roads.

a: SHORTEST PATH PROBLEM BASIC STATEMENT

The SPP searches for the shortest path between two vertices (one being the location of the EV (v_{ev}) and the other being the location of the previously selected point v_{in}) such that the sum of the weights of their edges is minimized by (9). The weight function $f : E \rightarrow \mathbb{R}$ has been adjusted to equal the length L_e of each edge $e \in E$, so $f = L_e$ showing that the chosen is based only on the shortest path, ignoring other costs.

$$Z_{B4} = Min \sum_{i=1}^{n-1}(D_{i,j})L_e \tag{9}$$

b: COMPUTATIONAL IMPLEMENTATION

The solution to this block was obtained using Algorithm 3. A previous step was added to the SPP to optimize resources, which consists of establishing a scan radius around each EV

($v_{ev} \in V_{EV}$) to create an initial set ($V_{IN} \in V_P$) of charging options (lines 1-10). Then, each v_i is compared with each $v_{in} \in V_{IN}$ using Euclidean distance, choosing the closest point. According to (10), the information is stored in an Euclidean Distance Matrix (EDM) [41].

$$D_{i,j}^2 = d_{i,j} \leftarrow \sqrt{(x_i - x_j)^2 + (y_i - y_j)^2} \tag{10}$$

Next, the SPP can be approached using the Single-Pair Shortest Path (SPSP) assumptions, i.e., looking for solutions between just one pair of vertices and not for the entire set G [38]. Dijkstra's algorithm was used for this solution in lines 11-18 [42]. The algorithm creates a shortest path tree, starting with an initial vertex and then exploring all its neighbors, updating the cost to reach each one. The set S is established to store the shortest paths, while the set Q holds the priority queue (used to store the unprocessed vertices). In lines 14-16, an iterative process extracts vertex u from Q and relaxes all adjacent edges of u. The algorithm continues until the target join is added to S, i.e., when the set Q is empty. Finally, in lines 19-21, the Algorithm 1 is again used to update the SOC of each vehicle between its stopping point and the destination charging point.

E. BLOCK 5: DEMAND ESTIMATE

Demand forecasting involves determining the approximate amount by which the electrical load will increase or decrease in the future, which is common in the operation and expansion planning of the electrical system [6], [23]. Traditionally, the goal has been to know how much energy is needed and when it is required. The demand must be frequently estimated because, among other factors, energy suppliers must meet any demand when it occurs [43]. For this reason, this block concludes the *X-Modeci*, with the aim of graphically and spatially identifying possible needs for reinforcements in the electricity grid, identifying critical periods during a typical day.

1) DEMAND AND COINCIDENCE

Generally, demand D is understood as the average of the electrical powers P (active or reactive) required by the load in a given time interval Δ_t according to (11) [44]. The demand at each charging point D_{CP} can be calculated by adding the individual demands of each EV according to equation (12). It has been calculated as the ratio between the amount of energy requested by the EV (given by the term that determines the difference between 80% of the battery capacity B and the value of its SOC when it arrives at the charge point SOC_{act}) by the time Δ_t. The value 0.8 is intended to limit charging to the maximum recommended by the manufacturer, as explained above.

$$D = \frac{1}{\Delta_t} \int_t^{t+\Delta_t} P(t) d_t(kW) \rightarrow \frac{P}{\Delta_t} \tag{11}$$

$$D_{CP} = \sum_{i=1}^{n} \left(\frac{[0,8B] - SOC_{act}}{\Delta_t} \right) \tag{12}$$

Algorithm 3 Stations and Routes Selection for SOC Update

Input: Location and SOC of each EV (V_P, Section IV-B2); EV Charging Infrastructure Location (V_{EV}, Section IV-C)

Output: Number of EVs at each EV-CI point; Updated SOC for each EVs

Implements: graph $G \leftarrow V, E, \mid V_P$ and $V_{EV} \in V$

1: $V_{IN} \leftarrow [\oslash]$
2: **for** Each ($v_{ev} \in V_{EV}$ **do**
3: **for** $v_p \in V_P$ **do**
4: Implements scan radius around $v_{ev} \in V_{EV}$ to find at least one
5: Select options found
6: Update V_{IN}
7: **end for**
8: Calculates euclidean distance with (9)
9: Selects the nearest point and stores it in $D_{i,j}$ weighted by L_e (10)
10: **end for**
11: $S \leftarrow [\oslash]$
12: $Q \leftarrow [V \in G]$
13: **while** $Q \neq 0$ **do**
14: Computes $Q \leftarrow Q - [u]$
15: **for** each $v \in Adj[u]$ **do**
16: Relax $[u, v]$
17: **end for**
18: **end while**
19: **for** each $v_{ev} \in V_{EV}$ **do**
20: Repeat lines 1-15 of Algorithm 1
 ⋮
21: **end for**
22: **return** Updated Dataframes

The coincident (or diversified) demand D_{coin} can be calculated by summing the individual demands of each consumer at time t [45]. This concept, applied to the proposal, gives (13), which can be used to show how loads are combined over some time. In addition, it is essential to know when the maximum demand of the set of loads occurs, which can be determined by the maximum coincident demand MD_{coin} according to (14). Furthermore, the sum of the maximum demands equals the maximum non-coincident demand MD_{Ncoin} according to (15). [46].

$$D_{coin} = \sum_{i=1}^{n} D_{CP}(t) \tag{13}$$

$$MD_{coin} = MaxD_{coin}(t_a) \tag{14}$$

$$MD_{Ncoin} = \sum_{i=1}^{n} MD_{coin} \tag{15}$$

2) TYPICAL FACTORS

In general, PDS studies are carried out with the help of indicators called typical factors, which show the

behavior of the load more clearly and quickly. Such factors are essential as they enable the sizing of installations (such as feeders or transformers, for example) and benefit the systematic monitoring of a given set. Among the many factors available, those most closely related to the proposed method are described and equated below [43].

a: DIVERSITY FACTOR

The ratio between the maximum non-coincident demand (MD_{Ncoin}) of a group of loads and the maximum coincident demand (MD_{coin}) of the set according to (16) [44]. The diversity factor is dimensionless and always ≥ 1. When $f_{div} = 1$, it is demonstrated that the maximum demands of all loads in a set occurred simultaneously.

$$f_{div} = \frac{MD_{Ncoin}}{MD_{coin}} \tag{16}$$

b: COINCIDENCE FACTOR (OR SIMULTANEITY)

The ratio between the maximum coincident demand (MD_{coin}) and the maximum non-coincident demand (MD_{Ncoin}) according to (17). Or, to put it more simply, it can be understood as the inverse of f_{div} [43]. The coincidence factor is dimensionless, $0 \leq f_{coin} \geq 1$. It indicates how much the maximum individual demand co-occurs with the maximum group demand. Consequently, f_{coin} decreases as the number of customers in a group increases, typically reaching a value between 0.5 and 0.33 [46].

$$f_{coin} = {f_{div}}^{-1} = \frac{1}{f_{div}} = \frac{MD_{coin}}{MD_{Ncoin}} \tag{17}$$

c: DEMAND FACTOR

It is the ratio between the maximum demand D_{max} and the total demanded demand C_{dem} (i.e., the nominal connected or total installed load) (18) [45]. The demand factor is also dimensionless, $0 \leq f_{dem} \geq 1$. In the proposed methodology, the demand factor informs how well the EV-CI is being used, indicating the percentage of installations in operation when maximum demand occurs [43].

$$f_{dem} = \frac{D_{max}}{C_{dem}} \tag{18}$$

d: LOAD FACTOR

The ratio between the average demand D_{med} and the maximum demand occurring in the same time interval according to (19) [44]. The load factor is dimensionless, $0 \leq f_{load} \geq 1$. It also indicates how well the installation is being used. When tending to 1, the more uniform the consumption is about demand; when closer to 0, the more variable the consumption is. When close to 1, it indicates that instantaneous demands throughout the day are close to maximum demand, that is, the peak [43].

$$f_{load} = \frac{D_{med}}{D_{max}} \tag{19}$$

V. CASE STUDY AND ANALYSIS

A. TEST DESCRIPTION

To illustrate the application of *X-Modeci*, the city of Salvador was chosen, located in the state of Bahia, in the north-eastern region of Brazil (coordinates $12.9777°S$, $38.5016°W$) [47]. It is the fourth largest metropolis in the country, with a population of around 3 million and a vehicle fleet estimated at over 1 million units. With an area of approximately 700,000 km^2, it is the 15th most significant metropolis in Brazil in terms of size.

All input data can be obtained free of charge from government websites, as they are public and widely used worldwide. For the selected location, socio-demographic data were obtained from the Brazilian Institute of Geography and Statistics (IBGE, by its Portuguese acronym) [48] and urban mobility data from the Municipal Department of Urban Mobility of Salvador (SEMOB, by its Portuguese acronym) [49].

Two global EV penetration scenarios were considered, 7% (scenario 1) and 65% (scenario 2). The choice of scenarios aims to emulate the current moment when penetration is still low (scenario 1) and a future moment when sales and EV-CI are more consolidated (scenario 2). In addition, technical data from the EVs Chevrolet Bolt [50] and Jac Motors iEV40 was considered [51]. The overall penetration rate refers to the percentage of EVs in the light vehicle fleet, where the portion for each model corresponds to half.

B. BLOCK 1 RESULTS

1) PRELIMINARY INFORMATION

A previous correlation analysis showed that the variables with the best correlation were 1) income (monthly income of permanent private households) and 2) housing (owned and paid for by permanent private households) [48]. The variables were updated for each year, considering an annual growth rate. According to Brazilian consumer behavior patterns, the premise was established that each inhabitant would allocate 30% of income to purchasing an EV and that the cost would be spread over time [48]. To be a potential adopter, the income earmarked for the purchase of the EV must be greater than the installment amount to be paid for the purchase.

2) RESULTS AND ANALYSIS

The results of this stage are obtained in a spatial database and can be visualized using heat maps as shown in Fig. 3. Darker shades denote sub-areas with higher adhesion; conversely, lighter shades show sub-areas with a lower purchase probability. The graduated bar next to the maps represents the probability, in *p.u.*, of a resident buying an EV in this area. In scenario 1 (Fig. 3a), there were 49,456 sub-areas with EVs; in scenario 2 (Fig. 3b), 364,285 were estimated.

In scenario 1 (Fig. 3a), the acquisition is low and predominantly in regions with higher social classes [48]. In addition

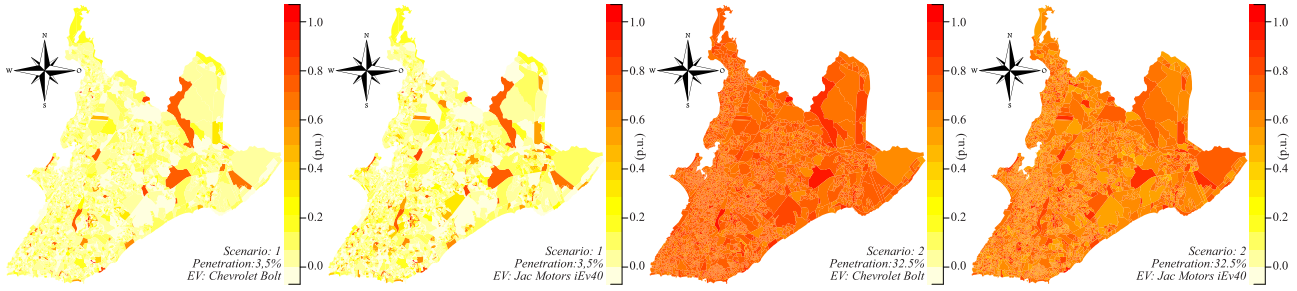

(a) Scenario 1 (07%) **(b)** Scenario 2 (65%)

FIGURE 3. Block 1 result: spatial distribution of global penetration of EV adopters in each scenario.

to the high initial cost, this phenomenon can be explained by other factors, including the lack of charging infrastructure, low battery autonomy, unreliable technology, and reach anxiety [25], [35]. Under these conditions, regions with zero adoption (blank areas) represent population conglomerates with lower purchasing power and worse quality of life indicators [48].

In scenario 2 (Fig. 3b), although it still represents a context in which electromobility is advancing, it's possible to realize the phenomenon of neighborhood influence (change in consumer behavior towards their peers) since a constant and gradual increase in the overall penetration rate is expected [26], [27], [37]. The areas with the highest take-up in scenario 1 (Fig. 3) have maintained their status and stimulated interest in the surrounding regions. As a result, areas surrounding those with more EVs behave in the same way and vice versa.

C. BLOCK 2 RESULTS

1) PRELIMINARY INFORMATION

In the study region, around 5,400,000 journeys are made on a typical day considering all transport modals (light vehicles account for approximately 20%) [49]. Several simulations in *Aimsun* (Section IV-B1) aimed to cover the busiest periods: morning peak, lunchtime, and afternoon peak. Journeys for motorbikes, trucks, and buses are fixed for all simulation periods. On the other hand, the trips made by conventional vehicles and EVs vary with each scenario to characterize the electrification effect of the fleet. Fig. 4 illustrates the traffic demand pattern in the study location.

a: INITIAL SOC RANGE

The EV's initial SOC (SOC_{int}, Section IV-B2), i.e., when it leaves its destination, is characterized randomly. During its journey, it is updated until it reaches its destination or until it reaches the minimum safety limit (SOC_{min}, set at 25%).

It is difficult to determine precisely the EV driver's behavior and movement patterns when charging is required. However, the range of the SOC_{int} has been configured as follows: at the start of the day, the SOC is closer to the maximum (80-100%); in the middle of the day, at medium levels (40-60%) and the end of the day at lower levels (25-40%). This behavior is also observed by [52], [53], and [54].

2) RESULTS AND ANALYSIS

The results are presented in thematic maps (Fig. 5 and Fig. 6), illustrating the distribution of the variables of interest along the roads in the study area. They have been pair-grouped with the mean flow and SOC for joint analysis. On the flow maps, warmer colors represent the busiest locations. Conversely, the warmer colors on the SOC represent locations where EVs are less loaded. The scales have been standardized in the same data distribution range to facilitate comparisons.

In Scenario 1 (Fig. 5), low penetration affects traffic intensity and is concentrated on main roads. Movement increases as the number of vehicles circulating in the region increases, which is expected [24]. In this sense, scenario 2 (Fig. 6) recorded the highest flow. The SOC variations evidence the initial random range assigned to each period (Section V-C1a). In the morning, for example, the predominantly green indicates that most EVs have sufficient charge for movement satisfactorily during the day.

a: SOC RANGE ANALYSIS

Fig. 7 illustrates the normal distribution of the results obtained from Algorithm 1, showing how the initial SOC (Section V-C1a) influences the results. It should be noted that between 06:00 and 08:00 AM, the EVs do not reach the minimum (SOC_{min}, adjusted at 25%). With an initial SOC range of 80 to 100%, EVs do not need to be charged, and this behavior is evidenced in the electrical demand calculation (Section V-F).

The inserted parameters show that, although there is a greater traffic flow in the morning, EVs with sufficient charge in their batteries predominate. Drivers depart, in general, from their homes with their vehicles already charged overnight using the home charging [52], [53], [54]. However, the distribution planner can adjust the initial range value to suit his reality and perform sensitivity analysis.

D. BLOCK 3 RESULTS

1) PRELIMINARY INFORMATION

When executing the Algorithm 2, the initial set of candidate locations is obtained considering all the costs (weighted

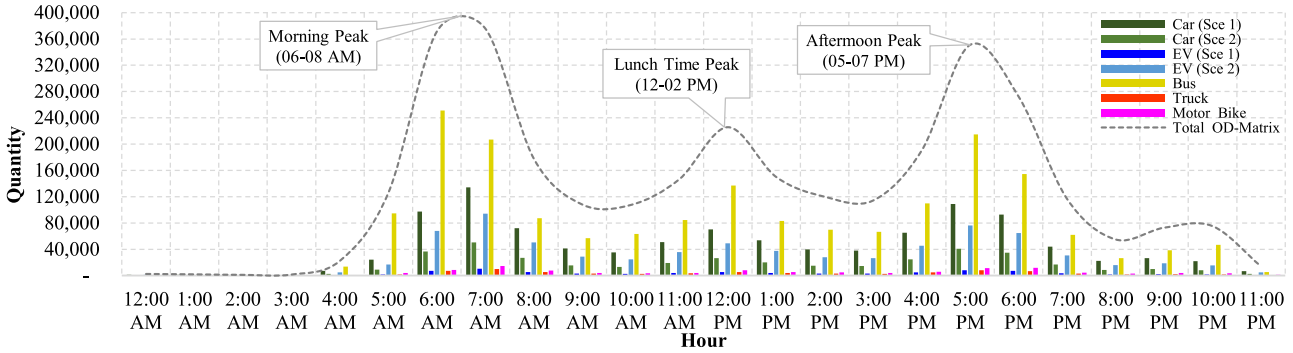

FIGURE 4. Traffic demand hourly curve for a typical day in the study region for traffic simulations [49].

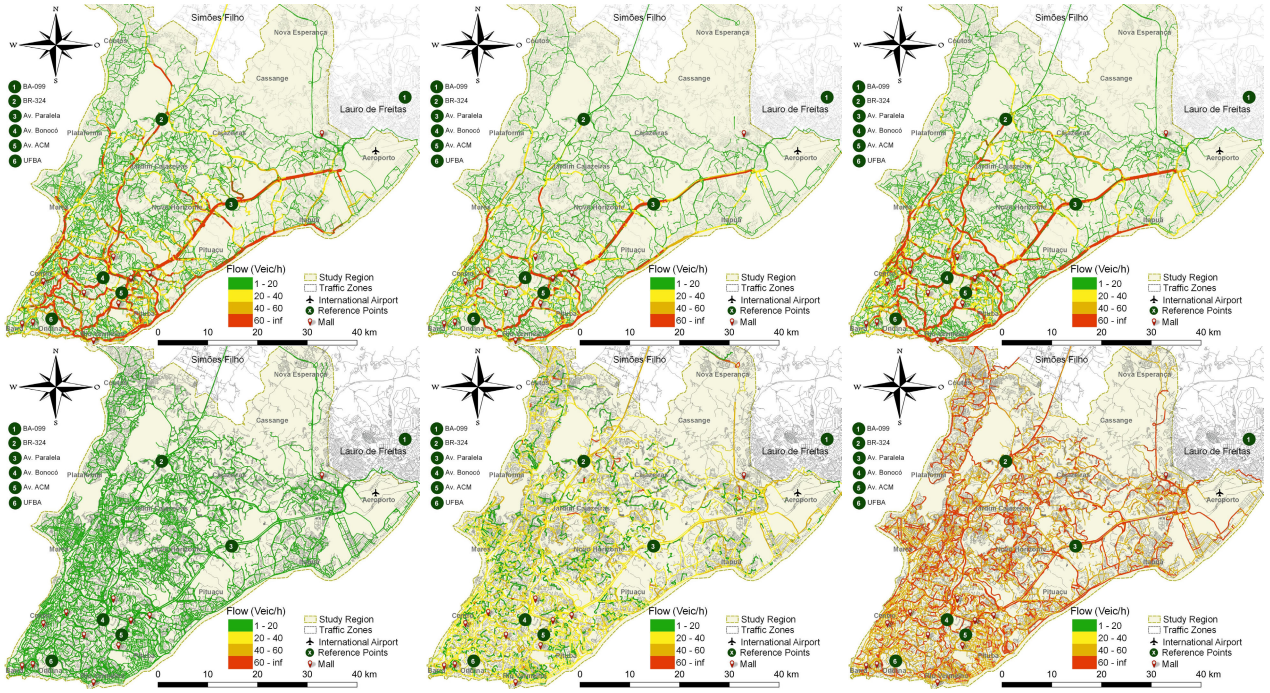

(a) 06h-08h AM (b) 12h-02h PM (c) 05h-07h PM

FIGURE 5. Block 2 result: average flow (above) and SOC (below) of electric vehicles on roads - scenario 1 (07%).

by (6)) to cover the demand. The algorithm only ends if at least one charging point attends all demands. The flow and SOC variables were adjusted by 10 and 20%, respectively, considering that promising locations for installation are those with high movement and low battery levels.

2) RESULTS AND ANALYSIS

The results for the two scenarios are shown in Fig. 8. The number of charging points proved adequate to meet the demand, being strategically positioned in places with easy access and heavy traffic, such as squares, commercial centers, shopping malls, etc. In scenario 1 (Fig. 8a), 46 points were allocated, while in scenario 2 (Fig. 8b), 249.

E. BLOCK 4 RESULTS

1) PRELIMINARY INFORMATION

This block aims to determine the number of EVs in each charging point and the SOC with which each one reaches it (SOC_{act}). The SOC_{min} was adjusted to a 25% of battery capacity for filtering vehicles needing charging.

2) RESULTS AND ANALYSIS

The results are presented for the two considered scenarios (Fig. 9 and Fig. 10), however eliminating the period from 06h-08h AM where, as justified in Section V-C1a (Fig. 6), the EVs have a satisfactory battery level. In graphs, the horizontal axis lists the identifiers (IDs) of the charging points. Average charging refers to the expected electricity consumption at each point, calculated by the sum of the difference between the batteries' residual energy and the value needed to reach 80% of their capacity. The total SOC refers to the sum of the energy remaining in the vehicles' batteries, in MWh, at each point. In all graphs, the three locations that received the most cars are highlighted with the notation *[Id of charging point; Number of vehicles at this point]*.

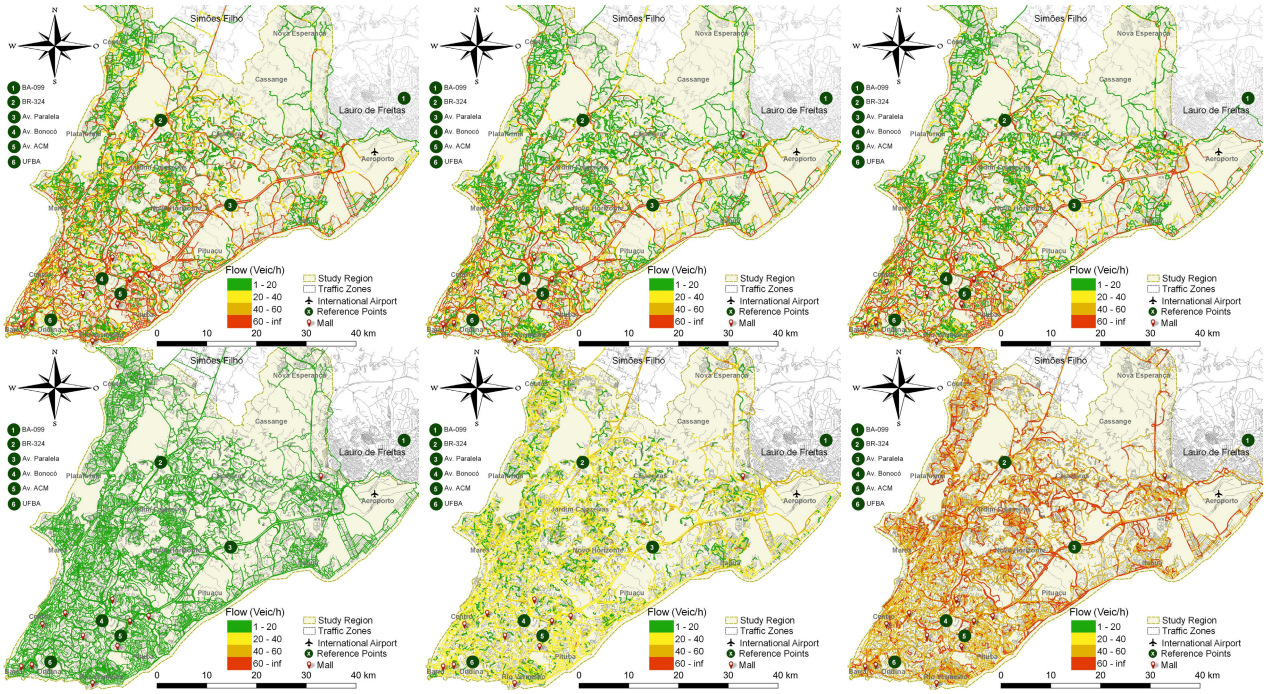

(a) 06h-08h AM (b) 12h-02h PM (c) 05h-07h PM

FIGURE 6. Block 2 result: average flow (above) and SOC (below) of electric vehicles on roads - scenario 2 (65%).

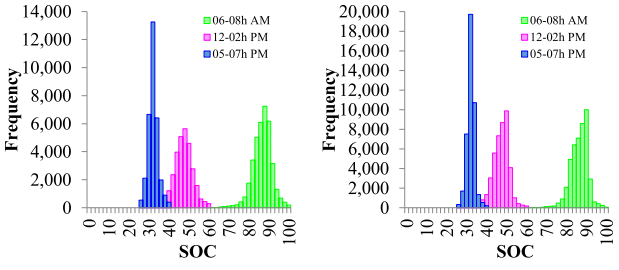

(a) Scenario 1 (07%) (b) Scenario 2 (65%)

FIGURE 7. Histogram of the SOC frequency distribution.

The results show that the period closest to the night is when more vehicles are looking for charging. This observation reflects the premise explained in Section V-C1a: on trips between 05:00-07:00 PM, it was considered that the SOC is at lower levels. Travel in this period is characterized by people leaving work or school and the end of business hours, which places great demand on the transport system [52], [54].

In scenario 1, 12h-02h PM (Fig. 9a), the charging points *ID25*, *ID46* and *ID1* received 46, 19 and 14 EVs, respectively. Fig. 9b shows that, between 05:00-07:00 PM, the *ID25* point received 424 vehicles, *ID35* received 409 and *46* received 384.

In scenario 2, 12h-02h PM (Fig. 10a), points *ID213*, *ID191*, and *ID200* received 239, 213 and 203 EVs, respectively. In Fig. 10b, point *ID213* received 2,630 vehicles, *ID180* received 1,421 and *ID114* received 1,317 vehicles.

TABLE 1. Summary of technical data of the analyzed charging stations.

Power (kW)	Current	Speed	Time (≈)
11	AC	Semi-Fast	4 hour
22	AC	Semi-Fast	2 hour
43	AC	Fast	1 hour
50	DC	Ultra-Fast	50 minutes
150	DC	Ultra-Fast	16 minutes

F. BLOCK 5 RESULTS

1) PRELIMINARY INFORMATION

Finally, this section analyzes the load curves and other electricity demand indicators. For the calculations, fast and ultra-fast charger models currently on the market were considered, as shown in Table 1 [22], [55].

2) RESULTS AND ANALYSIS

a: INDIVIDUAL (CHARGING POINTS)

The load curve (hourly demand) of each charging point and the coincident demand (D_{coin}) in each scenario are shown in Fig. 11. Multicolored lines represent the individual demand (kW) while the D_{coin} (MW) was plotted on the second axis (demarcated by the blue area). Both scenarios emphasized the demand peak at 5 PM, where a greater amplitude is observed in scenario 2 (65%), justified by the high penetration rate of EVs compared to scenario 1 (%07). At this time, D_{coin}, in scenario 1, reached 39.83 MW against 356.62 MW in scenario 2, an increase of 895.36%. This result confirms the

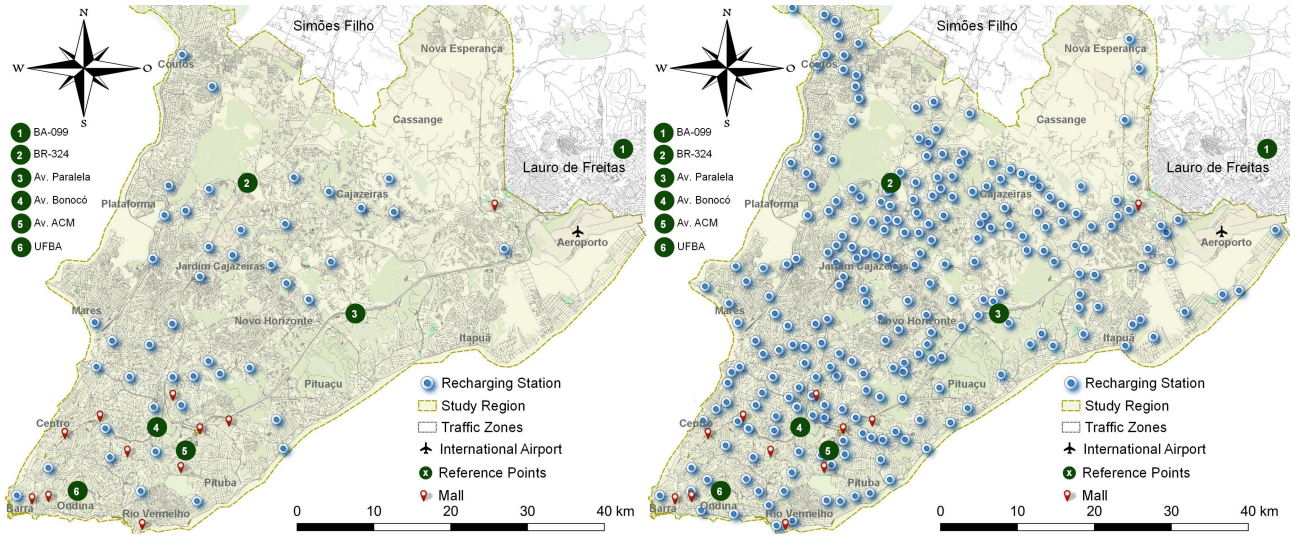

(a) Scenario 1 (07%) (b) Scenario 2 (65%)

FIGURE 8. Block 3 result: charging infrastructure estimation in each scenario.

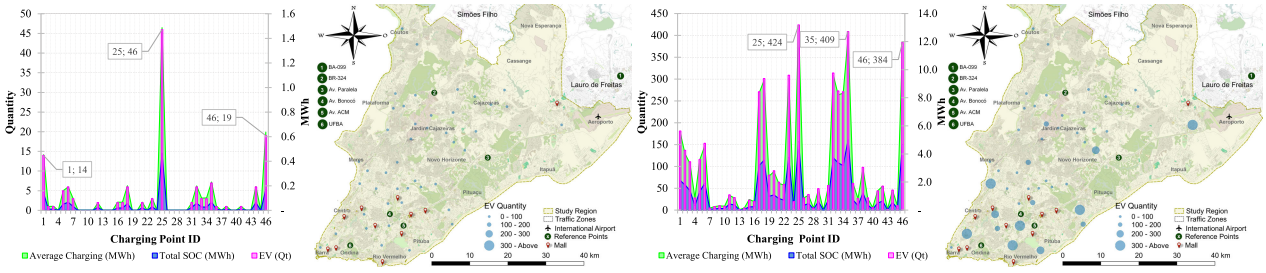

(a) 12h-02h PM (b) 05h-07h PM

FIGURE 9. Block 4 result: expected demand and spatial distribution of vehicles at each charging point - scenario 1 (07%).

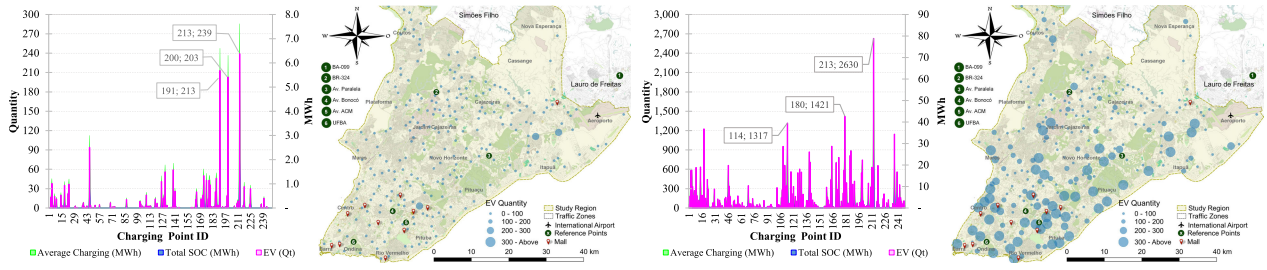

(a) 12h-02h PM (b) 05h-07h PM

FIGURE 10. Block 4 result: expected demand and spatial distribution of vehicles at each charging point - scenario 2 (65%).

understanding of many authors who justify that the public charging infrastructure tends to peak demand between late afternoon and early evening [52], [53], [54].

There was no registered demand between 01:00 AM (dawn) and 09:00 AM (morning). This fact demonstrates how sensitive the initial SOC range is (SOC_{int}, determined in Algorithm 1 and analyzed in Section V-C1a). According to established parameters, EVs have a satisfactory charge, preventing the search for an attractive charging service. Thus, the planner can vary this magnitude at the right time to create scenarios and sensitivity analyses, seeking an optimized configuration for the EV-CI.

From a PDS planning point of view, it is usual for the feeder to be sized for the maximum demand condition [44]. Therefore, Fig. 12 graphically and spatially shows its behavior. For scenario 1 (Fig. 12a), the highest peaks were at points *ID25*, *ID35*, and *ID46* whose values reached 3.7 MW, 3.4 MW, and 3.3 MW respectively. In scenario 2 (Fig. 12b), the peaks were at points *ID213*, *ID180*, and *ID114*, which reached 21.7 MW, 11.8 MW, and 11.0 MW.

Through the geographic location of the charging points and possession of the maximum demand of each one, the distribution planner can conduct connection studies. Data can help support decisions, aiming to choose a more

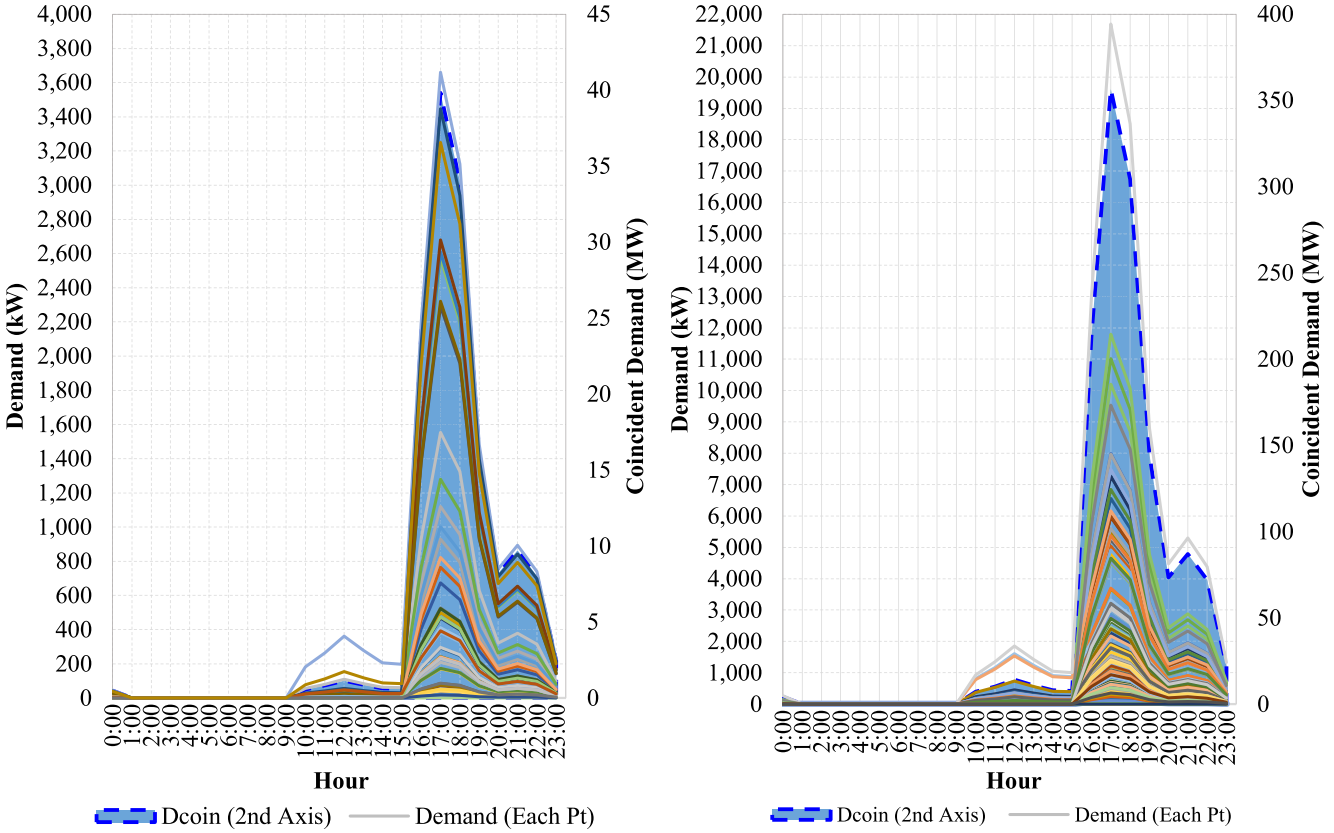

(a) Scenario 1 (07%)

(b) Scenario 2 (65%)

FIGURE 11. Block 5 result: hourly load curves for each charging point and coincident demand.

advantageous configuration from a technical/economic point of view. One can seek, for example, to minimize costs or maximize profits. Another advantage of associating demand with spatial location is the possibility of analyzing the consumer's profile, behavior pattern, and income, creating better-targeted marketing and customer acquisition campaigns.

Fig. 13 shows each scenario's load factor frequency distribution (from each charging point). This factor demonstrates how homogeneous energy use is and can assume a value between 0 and 1 where, the closer to 1, the more grouped the installation consumption [44]. The results confirm the previously reported behavior: high concentration of EVs charging simultaneously. As shown in Fig. 11, most EVs charge mainly at the end of the day, leaving the infrastructure little used or idle in other periods.

This result contributes to the entrepreneur or planner conducting campaigns with the public to fragment consumption at different times. It is often enjoyable for the distribution agent and the customer that consumption is diluted in off-peak periods [43]. From the distribution agent's point of view, this measure can mitigate/postpone reinforcements in the electrical grid; from the customer's point of view, the best energy use prevents higher charges caused by deviations between contracted and used demand (in the case of free consumers).

b: SET (INFRASTRUCTURE)

While in the previous section, the behavior of demand was individually analyzed (at each charging point), this section proposes an analysis of the entire infrastructure. Table 2 shows the main results. The maximum coincident and non-coincident demand (sum of the maximum demand of each point, which can occur at different instants of time) was the same for both scenarios. This fact also happened with the diversity and coincidence factors, indicating a large grouping of charges connected simultaneously in the system [45] and suggesting that all loads' maximum demands occurred simultaneously. As shown in Fig. 11, the parameters used for the case study showed a preference for charging at 5:00 PM in both scenarios. The load factor for the set also reflects this behavior, being similar because, during the early morning hours, the demand was considered null.

Regarding the demand factor of the set, its behavior was analyzed based on the variation in the use of the different powers of chargers of Table 1. The demand factor measures the relationship between the simultaneous use of charging points and the connected demand [44]. The results were better using 43 kW and 50 kW power chargers because they reached the recommended level (between 0.3 and 0.5) [46].

The analysis of the set shows that the large concentration of vehicles charging simultaneously impacted the demand and the factors analyzed. Assuming this to be a realistic situation,

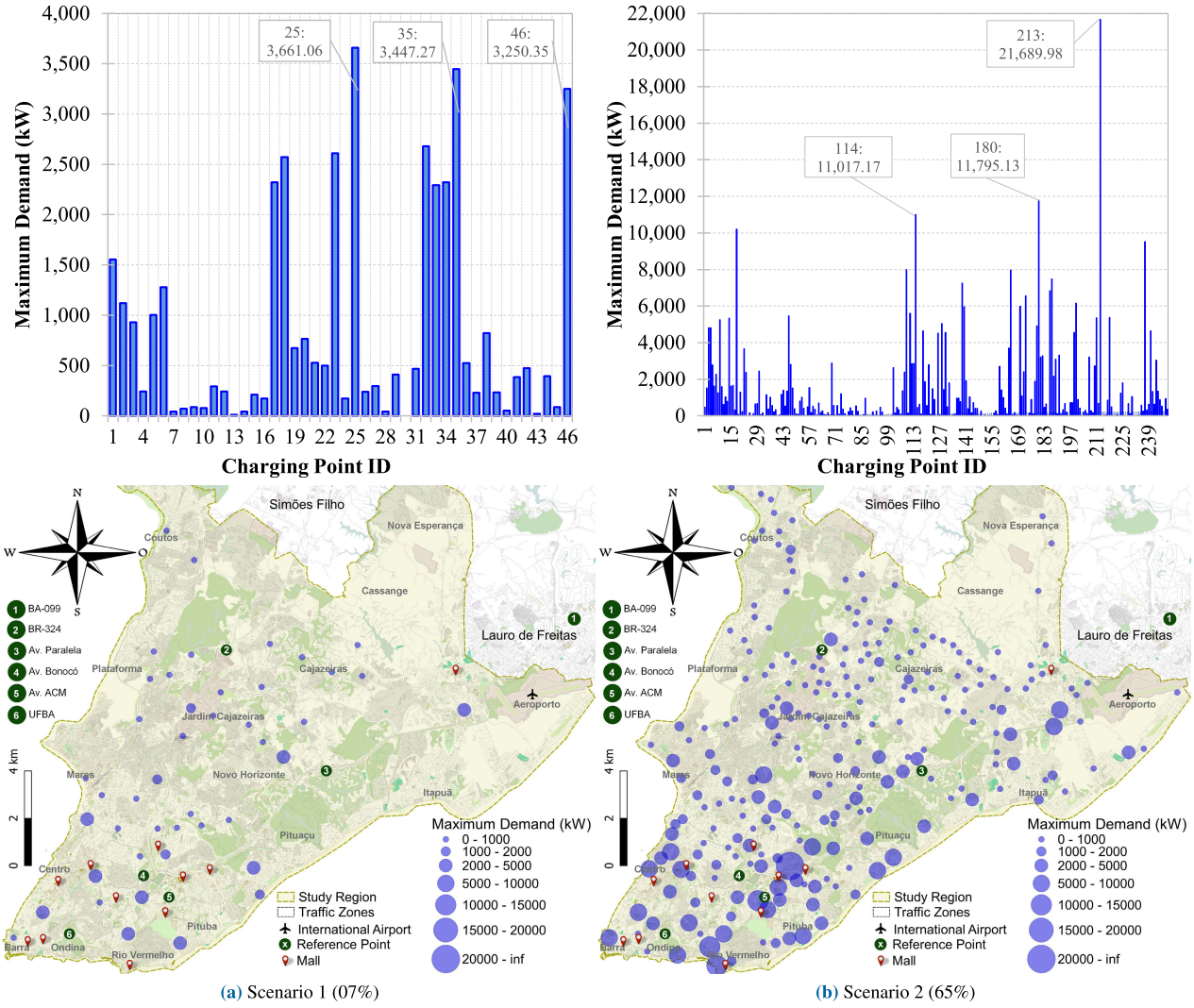

(a) Scenario 1 (07%) (b) Scenario 2 (65%)

FIGURE 12. Block 5 result: graphical and spatial analysis of the maximum demand at each charging point.

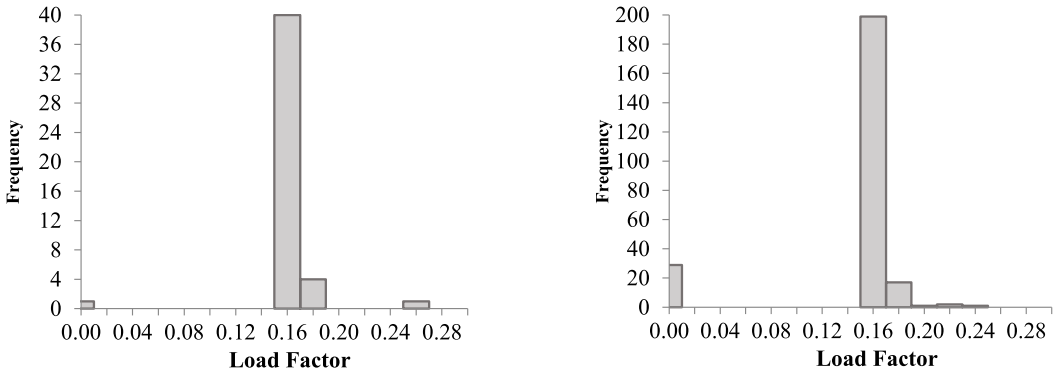

(a) Scenario 1 (07%) (b) Scenario 2 (65%)

FIGURE 13. Block 5 result: histogram of the load factor frequency distribution.

stakeholders should take collaborative measures to ensure the reliability of the power system, the sustainability of the businesses involved, and the adequate provision of services to the customer.

G. COMPARATIVE AND SENSITIVITY ANALYSIS

The *X-Modeci* has benefits over other recently released proposals (see the detailed comparison in the literature review in Section II). The most prominent contribution of

TABLE 2. Block 5 Result: summary of results for the entire infrastructure in each scenario.

Quantity	Symbol	Equation	Scenario 1	Scenario 2
Maximum Coincident Demand	MD_{coin}	(14)	39.83 MW	356.63 MW
Maximum Demand Not Coincident	MD_{Ncoin}	(15)	39.83 MW	356.61 MW
Diversity Factor	f_{div}	(16)	1	1
Coincidence Factor	f_{coin}	(17)	1	1
Load Factor	f_{load}	(19)	0.1541	0.1560
Demand Factor (11 kW Charger)			0.1873	0.1821
Demand Factor (22 kW Charger)			0.1873	0.1821
Demand Factor (43 kW Charger)	f_{dem}	(18)	0.3108	0.3022
Demand Factor (50 kW Charger)			0.3663	0.3561
Demand Factor (150 kW Charger)			0.1831	0.1781

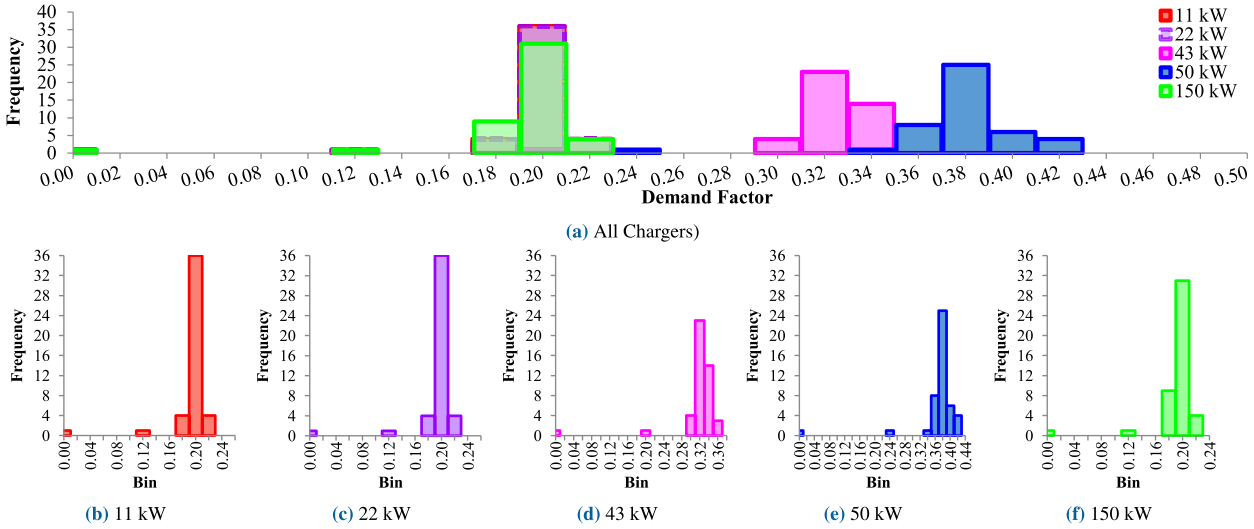

(a) All Chargers) (b) 11 kW (c) 22 kW (d) 43 kW (e) 50 kW (f) 150 kW

FIGURE 14. Sensitivity analysis: histogram of each charger's demand factor frequency distribution - scenario 1 (07%).

the proposal is the possibility of estimating load curves to assist distribution companies in connection analysis studies for new charging stations and in planning reinforcements in the electrical system infrastructure. In this sense, the *X-Modeci* stands out concerning others found in the literature by making it possible to characterize the growth of charge density in future scenarios.

In hypothesis, consider that a new enterprise of a charging station network requests the connection of 5 charging stations with a unit power of 100 kW each. Thus, the total nominal power of the new load is equivalent to a medium-sized industry or hospital, 500 kW or 625 kVA. With this information, the entrepreneur will request access to the distribution concessionaire that requires connection and hosting capacity studies, including local demand and feeder loading analysis. However, over the system expansion planning horizon (generally 3, 5, or 10 years), EV-CI will be expanded in a heterogeneous pattern, depending on the growth of the EV fleet. This will increase the demand with a pattern of behavior that is unknown and difficult to predict using traditional methods. In this sense, another benefit of the work about other proposals is the possibility of considering the different stages of EV adoption and use, improving the quality of the planner's analyses.

To better highlight the *X-Modeci* application for planning purposes, a sensitivity analysis was proposed involving the demand factor calculation and the five charger models considered in the case study (Table 1). The results are presented in Fig. 14 (scenario 1) and Fig. 15 (scenario 2). As detailed in Section IV-E, the demand factor is understood as the ratio between the maximum demand and the total installed load according to (18) [45]. The 50 kW charger (in blue) was proven more suitable in both scenarios. With this loader, there was a greater distribution of records with a demand factor close to 0.38 and 0.40, therefore within the ideal range (between 0.3 and 0.5) [46]. This result is justified because this charger allows for lower installed power and demand than the maximum demand at each charging point.

From an investment perspective, it is not economically viable to design an EV-CI to cover the demand for all EVs simultaneously. Charging tends to occur dispersed at different times of the day. Thus, the hourly distribution of the load contributes to reducing peak demand, reducing the initial investment cost. Furthermore, connecting a high power load

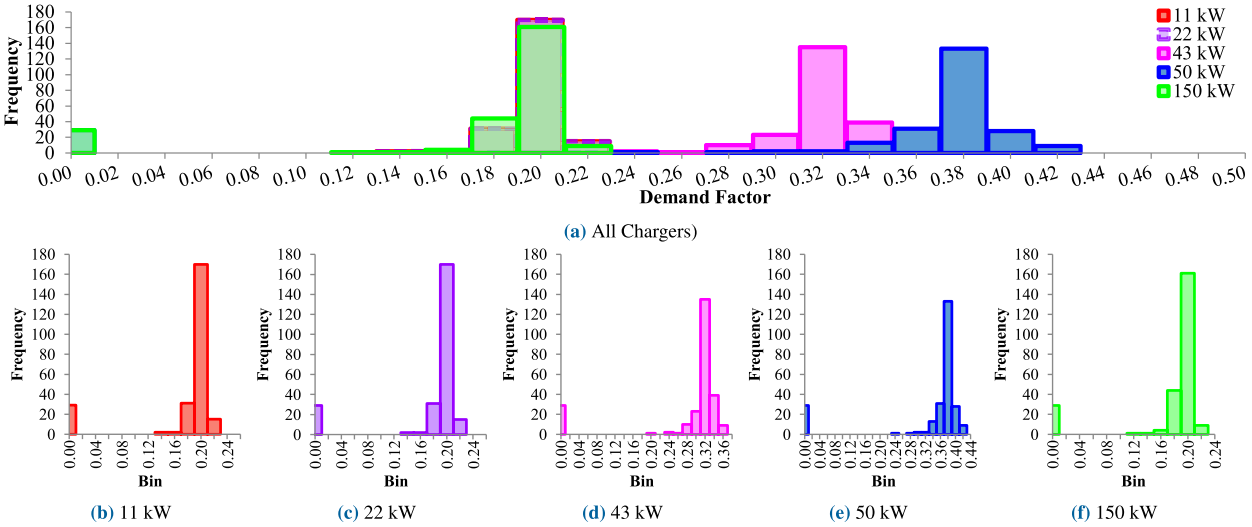

FIGURE 15. Sensitivity analysis: histogram of each charger's demand factor frequency distribution - scenario 2 (65%)).

to the distribution system may often require reinforcement work. In this sense, the better planned and used the structure, the lower the risk of system overload.

The *X-Modeci* was compared with the Brazilian reality, the country where the case study was prepared. Considering the most recent compiled data available [1], [26], [47], in 2022, the EV fleet was 40 thousand units, and the national EV-CI contained 1200 public charging points. Thus, the average proportion can be estimated as 1/33 (1 charging point for every 33 EVs). An established premise is that existing infrastructure is capable of satisfactorily meeting demand. The results obtained by the proposal reached a proportion of 1/36 in both scenarios analyzed. The *X-Modeci* brought a 10% gain in utilization, guaranteeing the supply of demand across the entire fleet and in compliance with the levels determined in the load curve and indicators (Section V-F). In other words, the hypothesis test shows that fewer chargers would need to be installed to meet the same demand.

VI. CONCLUSION

The present work presented an Extensive Mehod for Estimating Demand in Charging Infrastructures (*X-Modeci*) that aims to mitigate impacts related to uncertainties regarding the dynamism of growth in EV penetration and charging infrastructure. The method provides inputs for distribution companies to complement their analyses in the expansion planning stages or cases of requests for access to the electrical grid. The spatial database provided by *X-Modeci* can be integrated with power grid analysis tools, urban planning, land use mapping, topography, and others.

Significant differences exist in the trip distribution characteristics of EV drivers due to range anxiety and adopters' heterogeneous locations. From this perspective, trip-starting locations affect behavior, traffic dynamics, and, ultimately, the parameters of electrical demand.

Large volumes of traffic were observed in the morning and evening; however, significant loading occurred in the late afternoon and early evening, between 5:00 and 7:00 PM. The factors analyzed indicated a considerable simultaneous level, confirming a high concentration of EVs to be charged at the end of the day.

A sensitivity analysis compared five chargers models. The 50 kW nominal power model showed a more excellent distribution of records with a demand factor close to 0.38 and 0.40, therefore within the ideal range (between 0.3 and 0.5) [46]. Furthermore, *X-Modeci* brought a usage gain of 10%, compared to the standards for meeting charging demand of the current reality observed in Brazil (the study region). Demand for the entire fleet was met, taking into account maximum demand levels and load curves.

REFERENCES

[1] *Global EV Outlook 2024: Moving Towards Increased Affordability*, Int. Energy Agency, Paris, France, 2024. [Online]. Available: https://www.iea.org/reports/global-ev-outlook-2024

[2] M. Shafiei and A. Ghasemi-Marzbali, "Fast-charging station for electric vehicles, challenges and issues: A comprehensive review," *J. Energy Storage*, vol. 49, May 2022, Art. no. 104136. [Online]. Available: https://linkinghub.elsevier.com/retrieve/pii/S2352152X22001700

[3] S. Rahman, I. A. Khan, A. A. Khan, A. Mallik, and M. F. Nadeem, "Comprehensive review & impact analysis of integrating projected electric vehicle charging load to the existing low voltage distribution system," *Renew. Sustain. Energy Rev.*, vol. 153, Jan. 2022, Art. no. 111756. [Online]. Available: https://linkinghub.elsevier.com/retrieve/pii/S1364032121010273

[4] G. F. Savari, M. J. Sathik, L. A. Raman, A. El-Shahat, H. M. Hasanien, D. Almakhles, S. H. E. A. Aleem, and A. I. Omar, "Assessment of charging technologies, infrastructure and charging station recommendation schemes of electric vehicles: A review," *Ain Shams Eng. J.*, vol. 14, no. 4, Apr. 2023, Art. no. 101938. [Online]. Available: https://linkinghub.elsevier.com/retrieve/pii/S2090447922002490

[5] P. Farhadi and S. M. M. Tafreshi, "Charging stations for electric vehicles; A comprehensive review on planning, operation, configurations, codes and standards, challenges and future research directions," *Smart Sci.*, vol. 10, no. 3, pp. 213–245, Jul. 2022. [Online]. Available: https://www.tandfonline.com/doi/abs/10.1080/23080477.2021.2003947

[6] F. Ahmad, A. Iqbal, I. Ashraf, M. Marzband, and I. Khan, "Optimal location of electric vehicle charging station and its impact on distribution network: A review," *Energy Rep.*, vol. 8, pp. 2314–2333, Nov. 2022. [Online]. Available: https://linkinghub.elsevier.com/retrieve/pii/S2352484722001809

[7] A. J. Alrubaie, M. Salem, K. Yahya, M. Mohamed, and M. Kamarol, "A comprehensive review of electric vehicle charging stations with solar photovoltaic system considering market, technical requirements, network implications, and future challenges," *Sustainability*, vol. 15, no. 10, p. 8122, May 2023. [Online]. Available: https://www.mdpi.com/2071-1050/15/10/8122

[8] V. A. Martínez and A. Sumper, "Planning and operation objectives of public electric vehicle charging infrastructures: A review," *Energies*, vol. 16, no. 14, p. 5431, Jul. 2023. [Online]. Available: https://www.mdpi.com/1996-1073/16/14/5431

[9] T.-Y. Ma and Y. Fang, "Survey of charging management and infrastructure planning for electrified demand-responsive transport systems: Methodologies and recent developments," *Eur. Transp. Res. Rev.*, vol. 14, no. 1, p. 36, Dec. 2022. [Online]. Available: https://etrr.springeropen.com/articles/10.1186/s12544-022-00560-3

[10] F. J. Faustino, J. C. Lopes, J. D. Melo, T. Sousa, A. Padilha-Feltrin, J. A. S. Brito, and C. O. Garcia, "Identifying charging zones to allocate public charging stations for electric vehicles," *Energy*, vol. 283, Nov. 2023, Art. no. 128436. [Online]. Available: https://linkinghub.elsevier.com/retrieve/pii/S0360544223018303

[11] J. Chen and H. Chen, "Research on the planning of electric vehicle fast charging stations considering user selection preferences," *Energies*, vol. 16, no. 4, p. 1794, Feb. 2023. [Online]. Available: https://www.mdpi.com/1996-1073/16/4/1794

[12] C. Li, Y. Liao, R. Sun, R. Diao, K. Sun, J. Liu, L. Zhu, and Y. Jiang, "Prediction of EV charging load using two-stage time series decomposition and DeepBiLSTM model," *IEEE Access*, vol. 11, pp. 72925–72941, 2023. [Online]. Available: https://ieeexplore.ieee.org/document/10177923/

[13] S. Koohfar, W. Woldemariam, and A. Kumar, "Prediction of electric vehicles charging demand: A transformer-based deep learning approach," *Sustainability*, vol. 15, no. 3, p. 2105, Jan. 2023. [Online]. Available: https://www.mdpi.com/2071-1050/15/3/2105

[14] W. Huang, J. Wang, J. Wang, H. Zeng, M. Zhou, and J. Cao, "EV charging load profile identification and seasonal difference analysis via charging sessions data of charging stations," *Energy*, vol. 288, Feb. 2024, Art. no. 129771. [Online]. Available: https://linkinghub.elsevier.com/retrieve/pii/S0360544223031651

[15] L. Sica and F. Deflorio, "Estimation of charging demand for electric vehicles by discrete choice models and numerical simulations: Application to a case study in Turin," *Green Energy Intell. Transp.*, vol. 2, no. 2, Apr. 2023, Art. no. 100069. [Online]. Available: https://linkinghub.elsevier.com/retrieve/pii/S2773153723000051

[16] J. Feng, Z. Hu, and X. Duan, "EV fast charging station planning considering competition based on stochastic dynamic equilibrium," *IEEE Trans. Ind. Appl.*, vol. 59, no. 3, pp. 3795–3809, May 2023. [Online]. Available: https://ieeexplore.ieee.org/document/10012435/

[17] V. S. B. Kurukuru, M. A. Khan, and R. Singh, "Electric vehicle charging/discharging models for estimation of load profile in grid environments," *Electr. Power Compon. Syst.*, vol. 51, no. 3, pp. 279–295, Feb. 2023. [Online]. Available: https://www.tandfonline.com/doi/abs/10.1080/15325008.2022.2146811

[18] Y. Xing, F. Li, K. Sun, D. Wang, T. Chen, and Z. Zhang, "Multi-type electric vehicle load prediction based on Monte Carlo simulation," *Energy Rep.*, vol. 8, pp. 966–972, Nov. 2022. [Online]. Available: https://linkinghub.elsevier.com/retrieve/pii/S2352484722011106

[19] S. Das, P. Thakur, A. K. Singh, and S. N. Singh, "Optimal management of vehicle-to-grid and grid-to-vehicle strategies for load profile improvement in distribution system," *J. Energy Storage*, vol. 49, May 2022, Art. no. 104068. [Online]. Available: https://linkinghub.elsevier.com/retrieve/pii/S2352152X22001050

[20] L. N. F. D. Silva, M. B. Capeletti, A. D. R. Abaide, and L. L. Pfitscher, "A stochastic methodology for EV fast-charging load curve estimation considering the highway traffic and user behavior," *Energies*, vol. 17, no. 7, p. 1764, Apr. 2024. [Online]. Available: https://www.mdpi.com/1996-1073/17/7/1764/htm

[21] K. M. Tan, J. Y. Yong, V. K. Ramachandaramurthy, M. Mansor, J. Teh, and J. M. Guerrero, "Factors influencing global transportation electrification: Comparative analysis of electric and internal combustion engine vehicles," *Renew. Sustain. Energy Rev.*, vol. 184, Sep. 2023, Art. no. 113582. [Online]. Available: https://linkinghub.elsevier.com/retrieve/pii/S1364032123004392

[22] S. S. G. Acharige, M. E. Haque, M. T. Arif, N. Hosseinzadeh, K. N. Hasan, and A. M. T. Oo, "Review of electric vehicle charging technologies, standards, architectures, and converter configurations," *IEEE Access*, vol. 11, pp. 41218–41255, 2023. [Online]. Available: https://ieeexplore.ieee.org/document/10102467/

[23] J. M. B. Smith, K. Balasubramaniam, and R. Hadidi, "Assessing the need and state of power system and transportation system co-simulation," *IEEE Access*, vol. 11, pp. 44941–44951, 2023. [Online]. Available: https://ieeexplore.ieee.org/document/10119149/

[24] J. Barceló et al., *Fundamentals of Traffic Simulation* (International Series in Operations Research & Management Science), vol. 145, 1st ed., New York, NY, USA: Springer, 2010. [Online]. Available: http://link.springer.com/10.1007/978-1-4419-6142-6

[25] E. M. Rogers, *Diffusion of Innovations*, 3rd ed., New York, NY, USA: Free Press, 1983. [Online]. Available: https://www.simonandschuster.com/books/Diffusion-of-Innovations-5th-Edition/Everett-M-Rogers/9780743258234

[26] L. Bitencourt, B. Dias, T. Soares, B. Borba, J. Quirós-Tortós, and V. Costa, "Understanding business models for the adoption of electric vehicles and charging stations: Challenges and opportunities in Brazil," *IEEE Access*, vol. 11, pp. 63149–63166, 2023. [Online]. Available: https://ieeexplore.ieee.org/document/10155115/

[27] S. Fotheringham, C. Brunsdon, and M. Charlton, *Geographically Weighted Regression: The Analysis of Spatially Varying Relationships*, 1st ed., Hoboken, NJ, USA: Wiley, 2002. [Online]. Available: https://www.wiley.com/en-us/Geographically+Weighted+Regression%3A+The+Analysis+of+Spatially+Varying+Relationships+-p-9780471496168

[28] S. Shekhar, H. Xiong, and X. Zhou, *Encyclopedia of GIS*, 1st ed., New York, NY, USA: Springer, 2008. [Online]. Available: https://link.springer.com/referencework/10.1007/978-0-387-35973-1

[29] D. Hosmer, S. Lemeshow, and R. Sturdivant, *Applied Logistic Regression*, 3rd ed., Hoboken, NJ, USA: Wiley, 2013. [Online]. Available: https://onlinelibrary.wiley.com/doi/epub/10.1002/9781118548387

[30] Aimsun, Barcelona, Spain. (2021). *Aimsun Next 20: User's Manual*. [Online]. Available: https://www.aimsun.com/aimsun-next/download/

[31] J. de Dios Ortúzar and L. G. Willumsen, *Modelling Transport*, 4th ed., Chichester, U.K.: Wiley, Mar. 2011. [Online]. Available: http://doi.wiley.com/10.1002/9781119993308

[32] Open Street Map. (2024). *Map of the World*. [Online]. Available: https://www.openstreetmap.org/

[33] D. Goeke and M. Schneider, "Routing a mixed fleet of electric and conventional vehicles," *Eur. J. Oper. Res.*, vol. 245, no. 1, pp. 81–99, Aug. 2015. [Online]. Available: https://linkinghub.elsevier.com/retrieve/pii/S0377221715000697

[34] J. C. Lopes, T. Sousa, J. D. Melo, J. O. A. Torres, R. C. dos Santos, and P. T. L. Asano, "Electric vehicle SOC estimation on the roads of large cities employing traffic co-simulation and real mobility data," in *Proc. Workshop Commun. Netw. Power Syst. (WCNPS)*, Brasilia, Brazil, Nov. 2023, pp. 1–6. [Online]. Available: https://ieeexplore.ieee.org/document/10345219

[35] M. O. Metais, O. Jouini, Y. Perez, J. Berrada, and E. Suomalainen, "Too much or not enough? Planning electric vehicle charging infrastructure: A review of modeling options," *Renew. Sustain. Energy Rev.*, vol. 153, Jan. 2022, Art. no. 111719. [Online]. Available: https://linkinghub.elsevier.com/retrieve/pii/S136403212100993X

[36] P. Patil, K. Kazemzadeh, and P. Bansal, "Integration of charging behavior into infrastructure planning and management of electric vehicles: A systematic review and framework," *Sustain. Cities Soc.*, vol. 88, Jan. 2023, Art. no. 104265. [Online]. Available: https://linkinghub.elsevier.com/retrieve/pii/S2210670722005704

[37] R. S. Gupta, A. Tyagi, and S. Anand, "Optimal allocation of electric vehicles charging infrastructure, policies and future trends," *J. Energy Storage*, vol. 43, Nov. 2021, Art. no. 103291.

[38] L. Metcalf and W. Casey, "Graph theory," in *Cybersecurity and Applied Mathematics*, L. Metcalf and W. Casey, Eds., Boston, MA, USA: Syngress, 2016, ch. 5, pp. 67–94. [Online]. Available: https://www.sciencedirect.com/science/article/pii/B9780128044520000051

[39] S. L. Hakimi, "Optimum locations of switching centers and the absolute centers and medians of a graph," *Oper. Res.*, vol. 12, no. 3, pp. 450–459, Jun. 1964.

[40] M. B. Teitz and P. Bart, "Heuristic methods for estimating the generalized vertex median of a weighted graph," *Oper. Res.*, vol. 16, no. 5, pp. 955–961, Oct. 1968.

[41] I. Dokmanic, R. Parhizkar, J. Ranieri, and M. Vetterli, "Euclidean distance matrices: Essential theory, algorithms, and applications," *IEEE Signal Process. Mag.*, vol. 32, no. 6, pp. 12–30, Nov. 2015.
[42] E. W. Dijkstra, "A note on two problems in connexion with graphs," *Numerische Mathematik*, vol. 1, pp. 269–271, Dec. 1959, doi: 10.1007/BF01386390.
[43] W. H. Kersting, *Distribution System Modeling and Analysis*. Boca Raton, FL, USA: CRC Press, Aug. 2017. [Online]. Available: https://www.taylorfrancis.com/books/9781498772143
[44] T. Gönen, *Electric Power Distribution Engineering*, 3rd ed., Boca Raton, FL, USA: CRC Press, 2014. [Online]. Available: https://www.routledge.com/Electric-Power-Distribution-Engineering/Gonen/p/book/9781482207002#
[45] A. A. Sallam and O. P. Malik, *Electric Distribution Systems*, 1st ed., Hoboken, NJ, USA: Wiley, Apr. 2011. [Online]. Available: http://doi.wiley.com/10.1002/9780470943854
[46] H. L. Willis and W. G. Scott, *Distributed Power Generation*, 1st ed., H. L. Willis, Ed., Boca Raton, FL, USA: CRC Press, Oct. 2018. [Online]. Available: https://www.taylorfrancis.com/books/9781482263190
[47] Brazilian Institute of Geography and Statistics (IBGE). (2024). *Vehicles Fleet and Transportation Modes in Salvador, BA, Brazil*. [Online]. Available: https://cidades.ibge.gov.br/brasil/ba/salvador/pesquisa/22/28120
[48] (2024). *Statistics-Downloads: Structural Surveys, Sensuses, Among Others*. [Online]. Available: https://www.ibge.gov.br/en/statistics/downloads-statistics.html
[49] Municipal Department of Urban Mobility of Salvador (SEMOB),. (2024). *Salvador's Sustainable Urban Mobility Plan 2017*. [Online]. Available: https://planmob.salvador.ba.gov.br/
[50] Chevrolet. (2024). *New Chevrolet Bolt EV*. [Online]. Available: https://www.chevrolet.com/electric/bolt-ev
[51] JAC Motors. (2024). *JAC IEV40*. [Online]. Available: https://jacen.jac.com.cn/
[52] B. Borlaug, F. Yang, E. Pritchard, E. Wood, and J. Gonder, "Public electric vehicle charging station utilization in the united states," *Transp. Res. D, Transp. Environ.*, vol. 114, Jan. 2023, Art. no. 103564. [Online]. Available: https://linkinghub.elsevier.com/retrieve/pii/S136192092200390X
[53] D. Husarek, V. Salapic, S. Paulus, M. Metzger, and S. Niessen, "Modeling the impact of electric vehicle charging infrastructure on regional energy systems: Fields of action for an improved e-mobility integration," *Energies*, vol. 14, no. 23, p. 7992, Nov. 2021. [Online]. Available: https://www.mdpi.com/1996-1073/14/23/7992
[54] J. Zhang, Z. Wang, E. J. Miller, D. Cui, P. Liu, Z. Zhang, and Z. Sun, "Multi-period planning of locations and capacities of public charging stations," *J. Energy Storage*, vol. 72, Nov. 2023, Art. no. 108565. [Online]. Available: https://linkinghub.elsevier.com/retrieve/pii/S2352152X2301962X
[55] S. Thangavel, D. Mohanraj, T. Girijaprasanna, S. Raju, C. Dhanamjayulu, and S. M. Muyeen, "A comprehensive review on electric vehicle: Battery management system, charging station, traction motors," *IEEE Access*, vol. 11, pp. 20994–21019, 2023. [Online]. Available: https://ieeexplore.ieee.org/document/10056124/

JOSÉ CALIXTO LOPES (Member, IEEE) was born in Governador Valadares, Minas Gerais, Brazil. He received the degree in electrical engineering, in 2016, and the master's degree in electrical engineering and the Ph.D. degree in energy engineering from the Federal University of ABC, Santo André, Brazil, in 2020 and 2024, respectively.

From 2015 to 2017, he worked on research and consulting projects in Efficiency, Energy Planning, and Industrial Automation. Since 2018, he has been a Researcher with the Planning, Operation, and Regulation of Electric Power Systems Group, Federal University of ABC. His research interests include electromobility, energy efficiency, energy storage systems, power system planning, and renewable energy.

Dr. Lopes is an Associate Member of the IEEE Power and Energy Society and the International Council on Large Electrical Systems (CIGRE). He has received several national and state awards, including recognition from the Brazilian Association of Energy Conservation Services Companies (ABESCO) for the energy efficiency project presented to the Brazilian Congress on Energy Efficiency and others for its work in entrepreneurship and innovations, such as Google Techstar Startups, Hack Town SRS Startup Disruptors and the Engineering and Entrepreneurship Program of the National Confederation of Industry (CNI).

THALES SOUSA (Senior Member, IEEE) received the degree in electrical engineering from Paulista State University Julio de Mesquita Filho, São Paulo, Brazil, in 2001, the master's degree in electrical engineering from the Engineering School of Sao Carlos, University of São Paulo, São Paulo, in 2003, and the Ph.D. degree in electrical engineering from the Polytechnic School of the University of São Paulo, in 2006.

From 2003 to 2009, he was a Researcher with the University of São Paulo. Since 2011, he has been a Professor with the Federal University of ABC, Santo André, Brazil. He is the author of extensive bibliographic production that includes research and development projects, book contributions, and papers in internationally renowned journals and conferences. He has experience in electrical engineering, emphasizing electrical power systems. His research interests include operation, planning, and regulation of electric power systems.

Dr. Sousa is a Senior Member of the IEEE Power and Energy Society. He received the Award from the Brazilian Association of Electric Energy Distributors (ABRADEE) for the article presented at the National Seminar on Electric Energy Distribution.

JOEL D. MELO (Senior Member, IEEE) received the Bachelor of Science degree in electrical engineering from the Universidad Nacional Mayor de San Marcos (UNMSM), Lima, Peru, in 2006, and the master's and Ph.D. degree in electrical engineering from Universidade Estadual Paulista Júlio de Mesquita Filho (UNESP), Campus de Ilha Solteira, São Paulo, Brazil, in 2010 and 2014, respectively.

He is currently an Associate Professor with the Federal University of ABC, Santo André Campus, participating in developing research projects for electrical utilities. In his work experience, he worked in the mining company Shougang Hierro Peru (SHSAA) in electrical maintenance and electronic instrumentation for measuring electrical energy consumption and distribution substation protection, in 2007. In 2008, he became a Junior Professional at the control center of the transmission company power ISA-REP. In his scientific experience, he has been an Exhibitor and a Lecturer at scientific conferences, published in international journals, and a reviewer of scientific articles for these journals. His main research interests are in the areas of Electric Power Systems Planning and mainly in the application of spatial-temporal models to characterize the study area in the expansion planning process of the transmission and distribution systems.